Deanship of Graduate Studies
AL- Quds University

Detection of Trace Gas Emissions From Leaves, Seeds and Flowers Using Conventional and Photothermal Deflection Spectroscopy

Yasmeen Abdel Jaleel Mohammad Abu-Rayyan

M. Sc. Thesis

Jerusalem- Palestine

1430 / 2009

Detection of Trace Gas Emissions From Leaves, Seeds and Flowers Using Conventional and Photothermal Deflection Spectroscopy

Prepared by

Yasmeen Abdel Jaleel Mohammad Abu-Rayyan

B. Sc. Physics, Bethlehem University - Palestine

Supervisor: Prof. Dr. Mohammad Abu - Taha

"Thesis Submitted to the Faculty of Science, Al-Quds University in Partial Fulfillment of the Requirements for the Degree of Master of Science in physics"

Abu - Dies, Jerusalem

Palestine
1430 / 2009

Master Physics Program
Deanship of Graduate Studies

Detection of Trace Gas Emissions From Leaves, Seeds and Flowers Using Conventional and Photothermal Deflection Spectroscopy

Presented By:

Student Name: Yasmeen Abdel Jaleel Abu-Rayyan

Registration No.: 20411434

Supervisor: Prof. Dr . Mohammad Abu – Taha

Master thesis submitted for examination at 22 / 7 / 2009 and accepted by the examining committee as follows:

CommitteeMember		Signature
1- Prof. Dr . Mohammed Abu–Taha	Head of Committee	M Abu Taha
2- Dr. Rushdi Kitaneh	Internal Examiner	D. R. Kitaneh
3- Dr. Mustafa Abu-Safa	External Examiner	

Al – Quds University

1430/ 2009

DEDICATION

To my mother

To my father

To my husband

To my daughter

To my son

&

To my brother’s Mohamed soul

Yasmeen abdel Jaleel Mohammad Aburayyan

Declaration:

I certify that this thesis submitted for the degree of Master is the result of my own research, except where otherwise acknowledged, and that this thesis (or any part of the same) has not been submitted for a higher degree to any other university or institution.

Signed:…….

Name: yasmeen Abedl Jaleel Mohammad Abu- Rayyan

Date:

Acknowledgements:

Great thanks and prayer to Allah, who granted me the capability to finish this work.

I am grateful and thankful to my advisor Prof. Dr. Mohammad Abu – Taha for his assistance, kindness, and patience all the time during the research.

My great thanks to all my beloved family; to my mother who help me all time during my life are not forgettable, to my father for his support and to my sisters and brothers.

Special thanks go to my husband who was very patient and kind and supportive during my studies. My love and thanks to my daughter Rama and my son Yuseif.

Abstract:

Photothermal spectroscopy is a group of sensitive techniques used to study the optical absorption and thermal prosperities of the three material states, by detecting the difference in the deflection of probe beam position. Different kinds of position sensors were used for this aim. These sensors were sensitive but also expensive.

The present work concerned with the study of the effect of trace gases emitted from different samples on the path of the deflection laser probe beam. Two sensitive techniques were used, i.e. conventional light deflection (CLD) which is simple, inexpensive, easy to handle, and a more sophisticated photothermal deflection (PTLD) which employs expensive position sensors and rather more complicated than CLD.

The present work include a new experimental technique, simply a single slit with a photometer is used to investigate the light deflection position difference. The two methods proved their ability to distinguish different gas emissions.

ملخص:

مطيافية التأثير الضوئي الحراري هو مجموعة من التقنيات الحساسة المستخدمة في دراسة خصائص المواد بحالاتها الثلاث، عن طريق قياس التغير في موقع الشعاع الضوئي. تستخدم أنواع مختلفة من أجهزة قياس موقع الأشعة الضوئية، وهي أجهزة حساسة ولكنها أيضا مكلفة.

الدراسة الحالية تشمل دراسة تأثير الغازات القلية المنبعثة من عينات مختلفة على مسار شعاع الليزر المنعكس. واستخدم لتحقيق هذا الهدف طريقتين: طريقة انعكاس الضوء العادية ، وهي بسيطة وغير مكلفة ويسهل إتمامها. و الطريقة الثانية، هي التأثير الضوئي الحراري على مسار الشعاع المنعكس، وهي أكثر تطورا وتحتاج إلى جهاز قياس الموقع الغالي الثمن فهو أكثر تعقيدا من الطريقة الأولى.

العمل الحالي يشمل طريقة جديدة يمكن تجريبها وذلك باستخدام أدوات بسيطة مثل ال single slit و ال photometer المستخدم لقياس التغير في مسار الشعاع الضوئي.

هاتين الطريقتين أثبتتا قدرتهما على كشف انبعاث غازات مختلفة.

Table of Contents

Chapter one: Historical back ground:

1.1 Introduction……..……...……..……1
1.2 Statement of the problem……. ……..……..5

Chapter two: Theoretical background:

2.1. Introduction……..……...…….……6
2.2. Conventional light deflection ……..……..7
2.2.1. Refractive index ……...……...……...……8
2.2.2. Parameters that effects the refractive index …...…….…….……...9
2.3. Photothermal deflection ……..……..…….……10
2.3.1. The effect of temperature on the refractive index……...……..…10
2.3.2. Photothermal spectroscopy methods …….....……....11
2.3.2.1. Interferometry spectroscopy ……....12
2.3.2.2. Thermal lens spectroscopy …...……..…….....……12
2.3.2.3. Diffraction spectroscopy……..…...…...……13

2.3.3. Photothermal deflection spectroscopy (PTDS)…….….. ……..13
2.3.3.1. Principles of PTDS …….……...…..……14
2.3.3.2. Types of the PTLD technique……..…...……....……...20

2.4. Infrared (IR) spectroscopy……....21
2.5. The effect of other parameter on the light beam…...……...…….22
2.5.1. The effect of light absorption …….……..……..22
2.5.2. The effect of light scattering …….……..……..25

2.6. Detection of light deflection ……..……..……..…….27
2.6.1. Position sensor ……...……....…..……27
2.6.2. Diffraction method …….....……..…..……..29

Chapter Three: Experimental set up:

3.1. Introduction ……...…..……...…….……32
3.2. Equipment used for both experiments …….....……33
3.3. Conventional light deflection system …...……..……..……..33
3.4. Photothermal light deflection experimental system ……...…….……36
3.5. Wide band infrared source …….....……..……..……38
3.6. The photometer……...…...…...……..……...……...……..38

3.7. Detection scheme ……...……...……...…….40
3.8. Experimental set up ..……...…….40
3.9. Experimental samples ……..…..……42
3.9.1. Standard samples……..……..…….……42
3.9.2. Unknown samples …...……..……..…….43

3.10. Authentication of the experimental system ……..…..……..43
3.11. Conclusion ……...……..…...……43

Chapter Four: Results:

4.1. Introduction ……...…….……...…….44
4.2. Authentication of results …….....……..…….…….……45
4.3. Result of standardsamples……..……...……...……45
4.3.1. Intensity versus time signal …….……45
4.3.2. Methanol results ……..……...…….…….……46
4.3.3. Acetone results ……..…….……..……...……48

4.4. Unknown samples test ……..……..……...……...…....49
4.4.1. Leaves result (mint and sage)...……. ……....…… ……..49
4.4.2. Results for flowers (jasmine and rose) …....……...……53
4.4.3. Results for seeds (wheat and chick peas) ……..……57

4.5. Comparison between CLD and PTLD technique …….....……59

Chapter Five: Discussion:

5.1. Introduction ……...…….……...…….65
5.2. Conventional light deflection ……..……...……...……..66
5.2.1. Methanol and Acetone results ……..……...…..……..66
5.2.2. Leaves results …….....……...……..68
5.2.3. Flowers results …...……...…….……..69
5.2.4. Seeds results …...……..…….……70

5.3. PTLD results …….……....…….……..70
5.3.1. Methanol and acetone results …….……71
5.3.2. Mint results……...……72
5.3.3. Jasmine flower results ……...……...…….……...73
5.3.4. Chick peas results ……...……...……..……..74

5.4. Open area results ……..……..…….……75
5.5. Comparison results ……..…….....…..…….……75

Chapter Six: Conclusion and further work:

6.1. Introduction ……...…...……...…….……77
6.2. Further work……...……..78

References ……..……...……..…….……79

List of Figures:

Fig. No.	Fig. caption	Page
Fig.2.1	The four methods used for photothermal spectroscopy	**12**
Fig.2.2	The mirage effect (a) on hot desert (b) on cold water surface	**15**
Fig.2.3	Processes involved in photothermal spectroscopy	**15**
Fig.2.4	Absorption of light in a thin slice of matter of thickness Δx	**23**
Fig.2.5	Displacement of the reflected beam measured by a PSD	**27**
Fig.2.6	Measurement principle of rotation around a fixed point by a PSD	**28**
Fig.2.7	Photo of 2-D optical position sensor	**28**
Fig.2.8	Intensity distribution of diffracted light	**30**
Fig.3.1a	Schematic showing the conventional Light Deflection in the cell used to detect gas trace emissions from different samples.	**35**
Fig.3.1b	Photo showing the complete conventional light deflection experimental set up used to detect gas trace emissions from different samples.	**35**
Fig.3.2a	Schematic showing the PTLD experimental setup used to detect trace gas IR absorption	**37**
Fig.3.2b	Photo of the PTLD experimental setup used to detect trace gas IR absorptions.	**37**
Fig 3.3	Photo for the Pasco OS-8020 Photometer and its head	**39**
Fig.3.4	The relation between light intensity in (a.u.) and distance in (mm) from a center of the principle maxima	**41**
Fig.4.1a	Monitoring gas trace emissions of three different methanol's volumes using CLD technique.	**47**

Fig.4.1b	Monitoring gas trace emissions of three different methanol's volumes using PTLD technique	**47**
Fig. 4.2a	Monitoring gas trace emissions from different acetone's volumes using CLD effect technique.	**48**
Fig.4.2b	Monitoring gas trace emissions from different acetone's volumes using PTLD effect technique.	**49**
Fig4.3a	Monitoring gas emissions from two different crushed mint's masses using laser CLD technique.	**50**
Fig 4.3b	Comparison between gas emissions from 0.5 g crushed and uncrushed mint's leaves (rate of gas emission) using laser CLD technique.	**51**
Fig 4.4a	Monitoring gas emissions from two different crushed mint's masses using laser PTLD technique.	**51**
Fig 4.4b	Comparison between gas emissions from 0.5 g crushed and uncrushed mint's leaves (rate of gas emission) using laser PTLD technique.	**52**
Fig 4.5a	Monitoring gas emissions from two different crushed sage's masses using laser CLDtechnique.	**52**
Fig 4.5b	Comparison between gas emissions from 0.5 g crushed and uncrushed sage's leaves (rate of gas emission) using laser CLD technique.	**53**
Fig 4.6a	Comparison between white and yellow Jasmine flowers trace gas emissions using CLDtechnique.	**54**
Fig 4.6b	Comparison between crushed and uncrushed yellow Jasmine flowers trace gas emissions using CLD technique.	**55**
Fig 4.7	Comparison between white and yellow Jasmine flowers trace gas emissions using PTLD technique.	**55**
Fig 4.8a	Comparison between crushed and uncrushed white rose flowers trace gas emissions (rate of gas emission) using CLD technique.	**56**
Fig 4.8b	Comparison between crushed and uncrushed white rose flowers	**56**

	trace gas emissions (rate of gas emission) using CLD technique.	
Fig 4.9	Comparison between trace gas emissions from non contaminated and insect contaminated chick peas using CLD technique.	**57**
Fig 4.10	Comparison between trace gas emissions from non contaminated and insect contaminated chick peas using PTLD technique	58
Fig 4.11	Comparison between trace gas emissions from germinated and un germinated wheat grains using CLD technique.	58
Fig 4.12a	Comparison between the use of CLD and PTLD techniques to detect trace gases from 40µL of Methanol	60
Fig 4.12b	Comparison between the use of CLD and PTLD techniques to detect trace gases from 40µL of Acetone.	60
Fig 4.13	Comparison between the use of CLD and PTLD techniques to detect trace gases from 0.25g of mint	61
Fig 4.14	Comparison between the use of CLD and PTLD techniques to detect trace gases from jasmine white flower	61
Fig 4.15	Comparison between the use of CLD and PTLD technique to detect trace gases from insect contaminated chick peas.	62
Fig 4.16	Trace gas emissions from one Jasmine white flower using PTLD technique.	62
Fig 4.17	Detection of gas trace emission from jasmine's six (o.5g) plants' leaves using PTLD technique.	63
Fig 4.18	Comparison between the gas trace emissions from Jasmine's one flower and Jasmine's six plants' leaves (0.5g) using PTLD technique.	63
Fig 4.19	Comparison between the gas trace emission from 40µL of acetone and 40µL of methanol using CLD technique	64

List of abbreviations:

Symbol	Abbreviation representation
CLD	Conventional light deflection
PTLD	Photothermal light deflection
cw	Continuous wave
IR	Infrared radiation
PSD	Position sensitive detector

Chapter one

Historical background

1.1 Introduction.

This thesis is concerned with conventional and photothermal light deflection spectroscopy to detect the trace gases that are emitted from different types of samples. The light changes its speed when it passes from one transparent medium to another. This depends on the refractive index of the mediums. According to Snell's law (1591 - 1627) the relation between the refraction angle θ_2, angle of incidence θ_1 and the refractive index of the two mediums (n_1, n_2) is given as (Klein and Furtak, 1933):

$$\theta_2 = sin^{-1}\left(\frac{n_1}{n_2} sin\ \theta_1\right)$$

The velocity of light in any medium is smaller than in vacuum, this was first demonstrated experimentally for light propagating in water in the year 1850 by Foucault and Fizeau (Born and Wolf, 1959).

PTLD spectroscopy has been developed by Boccara and Fournier in 1980 and become an important tool for sub band gap absorption study in both films and bulk semiconductor materials (Chen,1993) and it becomes a sensitive technique to measure low absorption of different solid samples, thin films and optical coatings. By this technique the linear and non linear optical spectroscopic phenomena could be investigated. Boccara and Fournier studied the effect of the distance between pump an probe beams on the deflection and they used a position sensor to detect the deflected beam (Boccara and Fournier, 1980).

Now photothermal deflection technique is a successful method used to study some optical properties such as absorption spectra, thermal diffusivity…etc of the three material states; solid, liquid and gas (Havaux et al, 1989). Many Scientists used PTLD method to study different properties of the three material states and they using different kinds of position sensors. In 1980 Murphy and Aamodt used a position-sensitive silicon diode detector model SC-25 to detect the beam deflection to measure microwave absorption in liquids and to thermally heated liquid-solid interfaces (Murphy and Aamodt,1980). In 1989 Michel Havaux and Lucie Lorrain used a position sensor of Optikon SD 380-23-21-051 to monitor the photothermal deflection signals in vivo in leaves placed in various, liquid or gaseous, environments (Havaux et al, 1989). Zimering and Boccara used mirage effect to detect a real time in situ atmospheric trace gas. They used Centronic QD 50 –5T, a photodiode position sensor to monitor the deflection beam (Zimering and Boccara, 1996). In 1985 Sell used PTLD spectroscopy to study the gas velocity that could be measured by making the absorber gas concentration remained constant during the experiment and a lateral cell detector (silicon Detector Gorp. 386-22-21-251) was used to measure the deflection of the probe laser beam (Sell,1985). In 1997 PTLD technique was used to investigate the effect of O_2 incorporation into C_{60} thin films on the electronic structure by Tamihiro and others, they used a position sensor S3979 (Hamamatsu

Photonics) to detect the deflection beam produced by the optical absorption (Gotoh et al, 1997). In 1999 Shi measured the thermal diffusivity of boron- silicon film on glass configuration using the phase detection method of PTLD spectroscopy in transverse mode. The beam deflection was detected by Shi et al using a lock-in amplifier (Stanford Research system, model SR830) (Shi et al, 1999). The effect of the optical absorption by smoke from an acetylene diffusion flame on the signal was reported in 1990 by Pitz. This technique was used in, at first time by Rose and Gupta in 1982. Pitz used a lock-in amplifier referenced to the chopper frequency to detect the deflection beam; the lock-in output was linearly proportional to the absorber concentration (Pitz, 1990).

The two methods of PTLD, i.e. collinear and transverse methods, were used to study the optical prosperities of different materials, such as transverse phase of the PTLD method which was applied to measure the low thermal diffusivity of some materials in 1993 (Bertolotti et al, 1993), and the thermal diffusivity on solid samples was measured by Salazar and others using collinear PTLD method (Salazar et al, 1993).

In photothermal measurements, the detected signal depends on the temperature of the sample's surface and on its local optical absorption properties, which means that the 3-D heat flow does not significantly effect on the results obtained. In the 3-D heat flow study, sample's size and its geometry must be taken into consideration and heat flow near edges was used to study some properties of different samples (Aamodt and Murphy, 1982). So in 2002 Jyotsna Ravi and others evaluated the low thermal diffusivity of materials using PTLD spectroscopy (Ravi et al, 2002). Absorbencies of different DNA samples were studied in Al-Quds University using the well known photopyroelectric (PPE) technique. The photothermal figural was picked up and comprised with a Fourier Transform Infrared

(FTIR) spectrometer study. The absorbed radiation as a consequence generates a PPE signal which was picked up by a phase sensitive detector (Abu-Teir et al, 2008).

In this study the trace gases that are emitted from two evaporated materials are used to authenticate the use of the PTLD and conventional light deflection (CLD) methods. Following the confidence in system, six gas emitters of unknown gas structure with different volumes or masses were used to detect their gas emissions by both methods.

Brief review of thesis chapters: Chapter two of this study deals with the theoretical aspects of CLD and PTLD effects, and the discussion of IR spectroscopy. The effect of the optical absorption on the passage of the light beam will be discussed in this chapter as well. In chapter three the apparatus that were used in this study, experimental set up and experimental procedure are described. The experimental results will be given in chapter four, and their discussion presented in chapter five. Finally, the conclusion of this work and suggested further work are given in chapter six, which is followed by a list of references.

1.2 Statement of the problem

In PTLD method two laser sources were used; one as probe beam and the other as pump beam, and a position sensor was used to detect the light deflection as a result of gradient refractive index that produced from gas optical absorption.

In the present work there are new specific techniques which include:

1- Use single slit with a photometer to detect the light deflection instead of using expensive position sensor.

2- Use of wideband IR source instead of pump laser, allowing portable detection system to be constructed.

3- Use a simple theory of CLD method to detect trace gas emitted from different samples. This simple system doesn't need a lab.

4- Hold a comparison between results of CLD and PTLD methods.

5- Investigate the possibility of applying both methods in an open area.

Chapter two

Theoretical Background

2.1 Introduction

In this chapter, theoretical background of the main topics in this thesis are presented. The main part talks about the theory of CLD, which includes in formations about the refractive index and the effects of both gas density and temperature on the refractive index.

The second part talks about the theory of the PTLD spectroscopy, an introduction to the mirage effect is briefly reviewed. This is followed by an introduction to the types of the PTLD techniques. In addition, dependence of the deflection signal on various important parameters will be the main target of this chapter.

2.2 Conventional light deflection spectroscopy

The Conventional optical effect means that when light passes from one transparent medium to another, it changes speed, and bends. This depends on the refractive index of the mediums and the angle of incidence. In 1850, it was found by experiment that the speed of light in air is greater than in water, this result supported the wave theory of light suggested by Huygens and In 1621, a Dutch physicist Willebrord Snell (1591-1626), derived the relation between different angles of incidence and refraction as it passes from one transparent medium to another. This law often known as Snell's law, this statement was first given in terms of sins by Descartes 1637 (Serway, 1996).

$$n_1 \sin(\theta_1) = n_2 \sin(\theta_2) \qquad (2.1)$$

Where:

n_1: refractive index of the medium in which the incident ray travels.

n_2: refractive index of the medium through which the refracted ray travels.

θ_1: the angle (with respect to the normal) at which the incident ray strikes the boundary.

θ_2: the angle at which the refracted ray travels.

The idea of light bending toward or away from the normal drawn perpendicular to the line dividing the two mediums can act as a spectroscopic indicator, for example if light is passing in the same medium and in center part of it an index change does occur, then the beam change position accordingly confirming the change in the index, hence leading to a spectroscopic result related to the concerned medium.

2.2.1 Refractive Index:

The refractive index of a medium is a measure for how much the speed of light (or other waves) is reduced inside the medium. For example, typical glass has a refractive index of 1.5, which means that light travels at 1 / 1.5 = 0.67 times the speed in air or vacuum. Two common properties of transparent materials are directly related to their refractive index. First, light rays change direction when they cross the interface from air to the material, an effect that is used in lenses and glasses. Second, light is partially reflected from surfaces that have a refractive index different from that of their surroundings (Freeman, 1934).

An absolute refractive index of a medium is defined as the ratio of the velocity of a wave in vacum divided by the velocity in the medium. Thus

$$n = \frac{c}{v} \tag{2.2}$$

Where

n: absolute refractive index of a medium.

c: The speed of electromagnetic radiation in vacuum, it is approximately constant 3×10^8 m/s.

v: the phase velocity of radiation of a specific frequency in a specific material.

Example, the absolute refractive index of air is 1.00029.

The relative refractive index = $\frac{\text{velocity of light in one midum}}{\text{velocity of light in other midum}}$

$$n_{12} = \frac{n_2}{n_1} = \frac{v_1}{v_2} \tag{2.3}$$

The refractive index of the material changes with the wavelength of the light (Jenkins and Whith, 1937).

Maxwell determined the velocity of an electromagnetic wave from equation (4) as:

$$v = \frac{c}{\sqrt{\varepsilon\,\mu}} \tag{2.4}$$

Where:

ε: the material's relative permittivity.

μ : the material's relative permeability.

Comparison of equation 2 and equation 4 gives Maxwell's formula as:

$$n = \sqrt{\varepsilon\,\mu} \tag{2.5}$$

For most materials, μ is very close to 1(nonmagnetic substances) at optical frequencies, therefore (n) is approximately $\sqrt{\varepsilon}$. According to Newton, *n* depends on light frequency, so Maxwell's formula must be supposed that ε is a function of frequency (Born and Wolf, 1999).

2.2.2 Parameters that affects the refractive index:

The dependence of the refractive index (*n)* on the temperature and on the density (*ρ*) of the medium mathematically described by Lorenz-Lorenz relationship which is written as:

$$\frac{n^2-1}{n^2+2} = \frac{R_m}{m}\rho \tag{2.6}$$

Where:

R_m: the molar refractivity [m^3 mol^{-1}].

m: the molecular weight of the medium [kg mol^{-1}].

In the case of low pressures; below a few atmospheres and middling temperature the dependence of R_m on temperature can be neglected, so the refractive index is related to only the density change. For small temperature and density difference, the refractive index variated with the density changes can thus be written as:

(2.7)

By integrating equation (7) and considering that n≈1 at standard conditions, a linear dependence of the refractive index on the density can be obtained:

$$n_p = \frac{3}{2}\frac{R_m}{m}\rho \tag{2.8}$$

From this equation it is clear that the refractive index is directly proportional to the density (Calasso, 1998).

2.3 Photothermal light deflection (PTLD) spectroscopy

2.3.1 The effect of temperature on the refractive index:

In PTLD spectroscopy experiments a gradient in the refractive index is directly linked to thermal gradients as:

$$\nabla n = \nabla T \frac{dn}{dT} \tag{2.9}$$

Where dn/dT, the temperature coefficient of the refractive index, is considered to be inherent material parameter of the medium through which the probe beam passes. dn/dT could be contributed by two mechanisms; one is the medium thermal expansion which considers that the individual molecular polarizabilities within the material remain constant, and the other mechanism involves the thermal shift in the absorption bands of the medium. In PTLD spectroscopy a probe beam which is used must be chosen so that it's wave length doesn't account to absorption or scattering bands of the material, so that the second type of mechanism is negligible, and dn/dT can be attributed exclusively to expansion of the medium, so Lorenz-Lorenz relationship can hold (equation 2.6), and dn/dT can be written as:

$$\frac{dn}{dT} = \frac{1}{\rho}\frac{d\rho}{dT}(n^2-1)\frac{(n^2+2)}{6n} \quad (2.10)$$

If the probe is allowed to pass though gases (as in this study) which are free to expand without thermal stresses, the thermal expansion coefficient (β) will be written as:

$$\beta = -\frac{1}{\rho}(d\rho/dT) \quad (2.11)$$

So equation (2.10) becomes:

$$\frac{dn}{dT} = -\frac{\beta}{6n}(n^2-1)(n^2+2) \quad (2.12)$$

From this it is clear that dn/dT is directly proportional to thermal expansion coefficient. For example, for acetone; β =1.487 × 10^{-3} C^{-1} and n = 1.355 so dn/dT = -5.87 × 10^{-4} C^{-1}, and for methanol; β =1.199 × 10^{-3} C^{-1} and n = 1.325 so by equation (2.12) dn/dT = -4.28 × 10^{-4} C^{-1} (these two materials were used in our present study). For gases n is close to unity and by ideal gas law β = T^{-1}, so equation (10) simplifies to:

$$\frac{dn}{dT} \approx -\frac{(n-1)}{T} \quad (2.13)$$

The refractive index gradient can be obtained by obtaining the deflection of the probe beam (Spear and et al, 1990).

2.3.2 Photothermal spectroscopy methods:

The thermal state of the analytical sample can be monitored by using more than one method. For example, analytical sample temperature is directly measured by using calorimetric or thermometric methods employing temperature transducers. Photothermal spectroscopy belongs to a group of high sensitivity methods used to measure optical absorption and thermal characteristics of a sample by modulated index of refraction gradient resulting from the time dependent change in the medium temperature (Boccara and Fournier, 1980). The effect of the refractive index change on the passage of the probe

beam was studied by several methods. These methods are illustrated in Figure 2.1. Each method used to study a different physical quantity measured usually an amount or intensity of some parameters (Bialkowski, 1996).

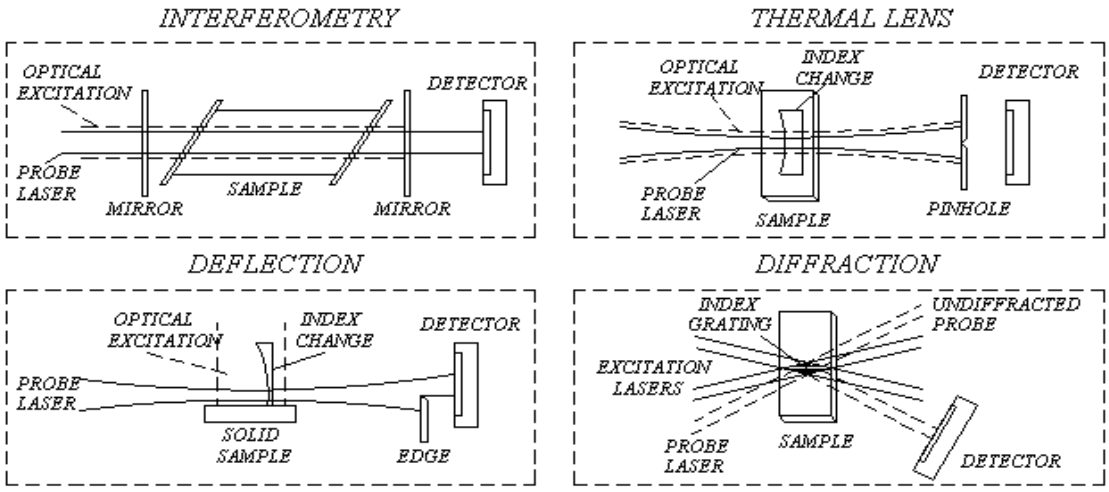

Fig.2.1: The four methods used for photothermal spectroscopy (After: Bialkowski, 1996).

2.3.2.1 Interferometric spectroscopy:

There are several different Photothermal Interferometriy methods used to detect the optical beam deflected induced by the photothermal effect (Kosmovskii, 1998). Interferometers operating with high spectral resolution at visible and infrared wavelengths method used to study the astrophysics and the physics of stars and circumstellar matter (http://www.springerlink.com/content/j137743836330278/,april 2009)

2.3.2.2 Thermal lens spectroscopy:

It is a photothermal effect and results when sample's temperature is increased as it absorbs the energy of a laser beam passing through the sample, the amount of heat depends on the laser wavelength and on the power of the laser. The result is a change in a refractive index that is proportional to the density and to the temperature resulting in formation of thermal

lens. Most materials expand upon heating, so that lens usually has a negative focal length. This negative lens causes beam divergence and the signal is detected as a time dependent decrease in power at the center of the beam (http://www.nsg.co.jp/en/it/c2/lens/tlm.html, April 2009). The method that is used to measure a signal induced by the combined effects of deflection and lensing called photothermal refraction spectroscopy.

2.3.2.3 Diffraction spectroscopy:

In diffraction method two beams are used as in PTLD spectroscopy; excitation and probe beams. So when the pump beam is absorbed by molecular species the temperature will increase associated with a change in the refractive index. In a diffraction method volume phase diffraction is a result of a periodic spatial refractive index modulation. Then the light diffracted at an angle that meets requirements from Bragg's Law. Amount of light diffraction is proportional to the refractive index change and measured by a photo electric detector, so this method measures the power of a beam diffracted by the periodic index (Bialkowski, 1996). In 1998 laser diffraction spectroscopy was used to describe a method of obtaining the size of human thrombocyte (Kosmovskii, 1998).

2.3.3 Photothermal deflection spectroscopy:

PTLD also named mirage effect is a sensitive technique suitable for measuring small values of optical absorption in different matters,. In PTLD two beams were used one as modulated heating beam which allowed normal incidence through the sample's surface, while the second probe beam runs either along the surface (transverse configuration) or along the heating beam (collinear configuration), for transparent sample. While the probe beam travels along the heated region it senses the modulated temperature gradient all its

path. Mirage effect has been extensively used to study the transport of heat, carriers, mass,...etc (Spear and et al, 1998). The PTLD could be used to detect a very low concentration of trace gases since it is very sensitive technique, and this sensitivity can lead to useful applications. For example, since the concentration of the absorbing molecules in the sample directly effect on the deflection of the probe beam, PTLD technique can be used to measure the concentration of the gas emission from different samples (Zimmering, and Boccara, 1997).

In this work photothermal deflection and light deflection spectroscopy are applied to detect the trace gases emission from the different mass or volume of liquid, flowers, leaves and seeds samples.

2.3.3.1: Principle of PTLD spectroscopy:

The phenomenon of the refractive index gradient can be seen in every day life. One famous example is the mirage effect; it causes the objects to be seen upright or upside down. Mirage is a phenomenon which occurs on hot sunny days when the air directly above the ground is hot so that its density decreases, resulting in a low refractive index. For example this effect occurs above flat asphalt which appear to be covered with pools of water, and in a hot desert, distant objects appear below the horizon as though in a pool of water. This effect may be seen on the beach, across firm and smooth sands. When the weather is warm and there is no wind and the water is much colder than the air above, a ship is seen to travel along the distant horizon upside down (Minnaert, 1974).

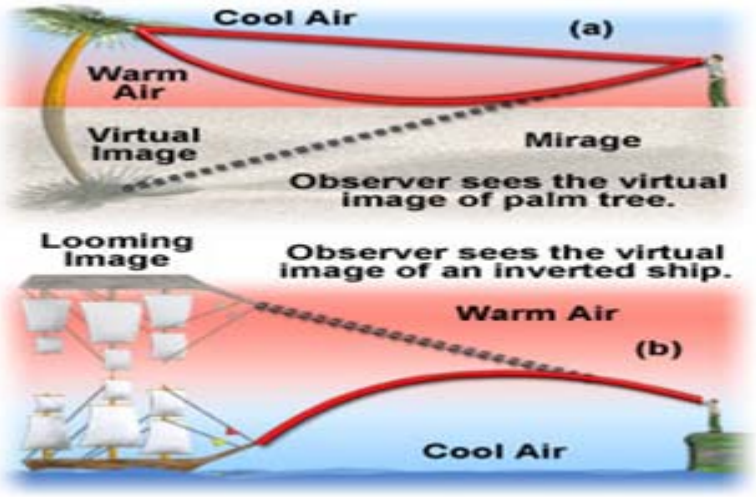

Fig.2.2: The mirage effect (a) on hot desert (b) on cold water surface (After: Sears, 1949).

The basic processes of PTLD technique can be described as in Figure 2.3. When the optical radiation is allowed to pass through the gas sample, hence as a result of energy absorption by gas molecules, this is followed by non radiative decay resulting in presurev and density gradients. Therefore a refractive index change is created in the heated region (Murphy and Aamodt, 1980).

Optical Excitation

⇩

Absorption

⇩

Excited state relaxation

⇩

Temperature change ⟺ Density change ⟺ pressure change
(Thermal diffusion) (Acoustic wave)

⇩

Optical probe ⟺ Refractive index change ⟺ photothermal signal

Fig.2.3: Processes involved in photothermal spectroscopy

(Redrawing after Bialkowski, 1996).

Absorption of radiation from the excitation source is modulated, this modulation is viewed as a modulation in the temperature gradient which is accompanied by pressure and density gradient and, thus, by a refractive index gradient that created in the heated region. The gradient of the varying refractive index can be monitored by a laser beam (probe beam) passing through the heated region.

Photothermal spectroscopy process can be broadly classified into two main areas that are discriminated based on physical phenomena used for temperature detection. In the first area, the optical absorption caused a thermal–induces change in the sample. This absorption produced heat that is monitored through mechanical action. The methods of photoacaustic spectroscopy and photothermal spectroscopes based on monitoring physical property changes are examples about this area. In the second area, the optical absorption caused a change in the refractive index which could be monitored by optical probes. The popular techniques of photothermal lens, photothermal deflection, and photothermal diffraction are examples about this area (Bialkowski, 1998).

In a prototypal photothermal experiment a sample excited with pulsed source (IR), as the excitation beam passes through the sample, it will be partially absorbed and this effect can be well-described by Beers law (De Vries, 1994).

$$P = P_0 \times 10^{-\alpha z} \tag{2.14}$$

Where:

α: the absorption coefficient of the sample.

Z: thickness of the sample.

P_0 and P: are the incident and transmitted power respectively.

When a molecule in the ground state absorbs a photon from incident radiation, this molecule may excite to the first excited state. When this molecule returned to its stable state its energy could be lost by radiative decay or by collisional decay. In IR range, collisional relaxation will occur because the quenching rates are sufficiently faster than radiative rates (De Vries, 1994).

The sample absorbabability can be characterized by a wavelength dependent optical absorption length A (λ) such that.

$$A(\lambda) = \frac{1}{\beta(\lambda)} \tag{2.15}$$

Where

β (λ): optical absorption coefficient. Part of absorbed energy released as

heat due to radiation loss process and the diffusion of heat produced by a pump source of modulation frequency f, through a gaseous sample of thermal conductivity κ, specific heat C, and density ρ can be represented by the thermal diffusion length

$$D(f) = \sqrt{\frac{\kappa}{\pi\rho c f}} \tag{2.16}$$

According to Coufal (1990), when the sample diffuses a distance of one thermal diffusion length D(f), only one diffusion length is significant as heat generated so a modulated excitation source produces a thermal wave of amplitude that is attenuated by a factor of $2x10^{-3}$ (Coufal, 1990). For effective deflection, the monitoring beam must probe the temperature gradient within one thermal diffusion length. This probe laser has a low power, low discharge voltage, and high stability. The angular deflection of the probe beam can be measured using a position sensor which is proportional to the intensity of the pump beam and to the concentration of absorbing sample's molecules (Bailey and Cruickshank, 1989).

If the sample is in contact with another medium, thermal waves are reflected and transmitted at the interface, and Equation (2.16) describing the heat diffusion extends into the second medium with the material parameters of that medium (Coufal, 1990). In photothermal spectroscopy when the pump beam was absorbed a temperature distribution is created and influenced by convection of the differential equation (17):

$$\frac{\partial T(\vec{r},t)}{\partial t} = D\nabla^2 T(\vec{r},t) - v_x \frac{\partial T(\vec{r},t)}{\partial x} + \frac{1}{\rho\, c_p} Q(\vec{r},t) \qquad (2.17)$$

Where:

$T(\vec{r}, t)$: the temperature distribution.

D: the thermal diffusivity of the sample in units of cm^2/s.

v_x: the slow velocity of the medium in the x-direction.

ρ: the density of the medium.

C_p: the specific heat at constant pressure of the medium.

$Q(\vec{r}, t)$: the temperature source term (w/cm^3), which is introduced by the absorption of the pump beam.

For continuous wave cw laser systems the term, Q(r, t) is given by equation (18):

$$Q(\vec{r},t) = \alpha I(\vec{r},t) = \frac{2\alpha P_{av}}{\pi a^2}[exp(-2r^2/a^2)](1 + cos\omega t) \qquad (2.18)$$

Where:

$I(\vec{r}, t)$: the intensity of the pump beam.

α: the absorption coefficient of an optically thin medium.

P_{av}: the average power of the pump beam.

a: the radius of the pump beam.

ω: the angular modulation frequency of the pump beam.

If the source term is known, the solution of equation (17) can be found, and the time-dependent temperature distribution inside the sample cell, is given by:

$$T(x,y,t) = \frac{2\alpha P_{av}}{\pi p c_p} \int \frac{1+\cos\omega\tau}{8D(t-\tau)+a^2} \exp\left(\frac{-2([x - v_x(t-\tau)]^2 + y^2)}{8D(t-\tau)+a^2}\right) d\tau \quad (2.19)$$

Where τ is the characteristic time. This temperature distribution generated a time–dependent refractive index gradient inside the cell, which is described by:

$$n(x,y,t) = n_0 + \frac{\partial n}{\partial T} T(x,y,t) \quad (2.20)$$

Where:

n(x, y, t): the refractive index inside the cell.

n_0 : the refractive index at the ambient temperature (Malik and Faubel, 2000).

To obtain maximum sensitivity, the PTLD instrument is operated in the low frequency regime. In this case, the thermal diffusion length D (*f*) which is given by the expression in Equation (16) is much greater than the probe beam diameter (D (*f*) >>a).

For low modulation frequency, small deflection angles and a pump beam with a Gaussian profile, the angular deflection of the probe beam in radians is

$$\Phi = \frac{dn}{dT} \frac{P_0}{\pi^2 k x_0} \left[1 - exp(-\alpha l)\right]\left\{1 - exp\left(\frac{-x_0^2}{a_0^2}\right)\right\} \quad (2.21)$$

Where:

$\frac{dn}{dT}$: Temperature coefficient of the index of refraction of the medium

l: the beam crossing length

x_0: the separation distance between the centers of the pump and probe beams.

For small αl (<2), the deflection amplitude is proportional to the optical absorption and to the power while inversely proportional to the modulation frequency. Φ exhibits maximum near $(x_0/a_0) \sim 1$ (Boccara and Fournier, 1980).

In the case in which the thermal diffusion length is much larger, or where the medium has a low thermal diffusivity (D (f) <a), the deflection angle is given by

$$\Phi = 2\left(\frac{1}{n_0}\frac{dn}{dT}\right)\left(\frac{x_0}{a^4}\frac{P_e}{\omega_p c n^2}\right)[1 - \exp(-\alpha l)]\left\{\exp\left(\frac{-x_0^2}{a_0^2}\right)\right\} \quad (2.22)$$

(Zimmering, and et al, 1997).

2.3.3.2 Types of the PTLD Technique:

Theories of the PTLD technique can be categorized according to the type of the pump laser used to excite the sample. The deflection of a cw laser probe beam caused by the refractive index variation depends on the employed PTLD scheme. The PTLD technique is generally applied in both, the parallel and the transversal pump-probe beam configuration (Bialkowski, 1996, Boccara and Fournier, 1988).

A cw PTLD theory, when the pump laser is a cw one has two techniques type;

1. Collinear PTLD technique, in which the probe and pump beams are parallel. In this case, the gradient of the refractive index is both created and probed within the sample (Salazar et al, 1993).

2. Transverse PTLD technique, in which the probe beam is perpendicular to the pump beam, and in this case, the refractive index gradient is generated in a thin layer adjacent to the sample (Bertolottii, 1993).

2.4 Infrared (IR) Spectroscopy

IR spectroscopy was discovered by Sir William Herchel, it is important because of the high information content of a spectrum and because of its variety of possibilities for sample analysis and substance preparation. The heat absorbed is the result of irradiation infrared laser, and it is a useful technique for the characterization of organic materials. The position and intensity of absorption bans of substance are extremely specific like a finger print of a person.

The advantages of IR technique are:

1. IR spectroscopy allows subwavelength resolution and uses a variant of photothermal displacement spectroscopy.
2. This technique is sensitive to study particles that are having the ability to attenuate interfering absorption from the supporting substrate.
3. This technique is used in the analysis of weakly absorbing systems.
4. This technique is nondestructive, does not require vacuum, and is usable on a variety of surfaces and thin films (Gunzler and Gremlich, 2002).

The temperature attained by the material is proportional to the absorption coefficient of the material at the pump wavelength. The displacement of a photothermal approximately is given by:

$$h = \beta \, \Delta T \, L_{eff} \tag{2.23}$$

β: is the thermal expansion coefficient of the material.

ΔT: is the average temperature modulation over an effective length fraction (L_{eff}).

L_{eff}: depends on the thermal diffusion length, the optical absorption length, the depth of the absorber below the surface, the absorber size, and the elastic properties of the material.

A simple analysis of the thermal response of a particle to a modulated heat source is found by Utterback et al (Taubenblatt, 1988)to be

$$\Delta T = \left(\frac{P_0/G}{1 + i\,\omega\rho\, CV/G}\right) exp(i\omega t) \qquad (2.24)$$

Where:

G: is the conductivity to the surrounding media.

P_o: is the power absorbed by the particle.

V: is the volume.

C: the heat capacity of the particle.

Experimentally it is found that G depends on the particle radius and the power absorbed by a small particle is proportional to (α I_0V)

Where:

α: is the wavelength-dependent absorption coefficient of the material.

I_0: is the incident IR intensity.

2.5 The effect of other parameters on the light beam

2.5.1 The effect of light absorption:

Absorption spectroscopy is a comparison technique between the power of a beam of light before and after interaction with a sample. When a light of a continuous wavelengths (cw) passes through gas samples, part of this radiation may be absorbed, reflected or transmited by the sample's molecules. When sample's molecules absorb a photon from incident radiation, photon's energy will be transformed to other form of energy, for example heat energy. The absorpted energy depends on the radiation frequency and on the natural of the sample's atoms which contain electrons attached to them, these electrons are vibrated at

specific frequencies. The frequency at which an object vibrates is given by the following equation:

$$f = \frac{v}{\lambda}$$

Where:

f: frequency, c: the velocity, : the wavelength.

If the incident radiation of a given frequency strikes a material, electrons will absorb the energy of the light wave and starts a vibrational motion. During this motion, the electron interacts with neighboring atoms in such a manner as to convert its vibrational energy into thermal energy (Lajunen, 1992).

Not all photons get absorbed, it is related to other properties of the sample; assume that the light pass through a thin slice of material of thickness Δx (Figure 2.4).

Then $\Delta P = P_0 - P$, and the magnitude of this loss is proportional to P_0, to thickness, and to the absorptivity (α).

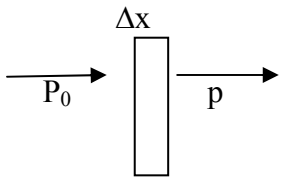

Fig.2.4: Absorption of light in a thin slice of matter
of thickness Δx (Redrawing after Arendt, 1989)

$$-\Delta P = P_0 \, \alpha \, \Delta x \qquad (2.25)$$

$$\frac{\partial P}{P_0} = -\alpha dx \Rightarrow \int_{P_0}^{P} \frac{\partial P}{P_0} = -\alpha \int_0^x dx$$

$$\ln \frac{P}{P_0} = -\alpha x \qquad (2.26)$$

As Beer-Lambert states, there is a logarithmic dependence between the transmission (T) of light and the product of the absorption coefficient (α) through a substance, for gases the

relation is given as:

$$T = \frac{P}{P_0} = 10^{-\alpha x} = 10^{-\sigma x c} \quad (2.27)$$

Where

P_0:the power of the incident on beam the material and P is the power that emerges from it.

σ: an absorption cross section.

c: the concentration of the solution (grams or moles / liter).

α: absorption coefficient and it is one of many ways to describe the absorption of electromagnetic waves. α can be expressed in terms of the imaginary part of the refractive index, κ, and the wavelength of the light λ_0, according to:

$$\alpha = \frac{2\pi k}{\lambda_0} \quad (2.28)$$

Where: k is the extinction coefficient, which indicates the amount of absorption loss when the electromagnetic wave propagates through the material.

The transmission is expressed in terms of an absorbance which for gases is defined as:

$$A = -\ln T = -\mathrm{Ln}\frac{I}{I_0} \quad (2.29)$$

This implies that the absorbance becomes linear with the concentration according to:

$$A = \alpha x = \sigma x c \quad (2.30)$$

Thus, if the path length and the molar absorptivity (or the absorption cross section) are known and the absorbance is measured, the concentration of the substance can be deduced (Arendt, 1989).

2.5.2 The effect of light scattering:

When light hits small particles the light scatters in all directions, and if these particles are much smaller than the incident light wavelength, this scattering will be a Rayleigh scattering. Such as the scattering of the light when it travels in transparent solids, liquids, and mostly in gases. Rayleigh scattering in clear atmosphere is the reason why the sky is blue (Stover, 1995). By dividing the particle characteristic dimension (r) onto light radiation wavelength λ, the scattering particles siz is given as:

$$x = \frac{2\pi r}{\lambda} \tag{2.31}$$

From this relation it is clear that the light scattering can be defined as a Rayleigh scattering when x<<1, this since in Rayleigh scattering r << λ. The amount of Rayleigh scattering depends on the wavelength of light, the size of the particles, the scattering coefficient, and on the incident light intensity. So when a beam of wavelength λ and intensity I_0 scattered by a single small particle, its intensity I is given by equation (2.30):

$$I = I_0 \frac{1+\cos^2\theta}{2R^2}\left(\frac{2\pi}{\lambda}\right)^4\left(\frac{n^2-1}{n^2+2}\right)^2\left(\frac{d}{2}\right)^6 \tag{2.32}$$

Where:

R: the distance to the particle.

θ: the scattering angle.

d: the diameter of the particle (Bohren and Huffman, 1983).

In collinear PTLD if a probe and pump beams diameters and the thermal diffusion length of the modulation excitation beam D (f) are much smaller than the thickness of the sample Z, the power of the excitation beam passing through the sample will be reduced exponentially with an extinction coefficient equal to the sum of it's scattering coefficient α_s, and absorption coefficient α_a.

When a photon from the excitation beam is scattered it may be absorbed by the sample in a region $1/\alpha_a$ far away from its original path. Since α^{-1} is much greater than the pump or probe beam diameters, the thermal gradient produced may not be sampled effectively by the probe beam since the absorption process does not occur near a region through which the probe beam propagates, thus, it can degrade the mirage signal. However this influence can be represented by means of a clarity factor (C.F.), which was defined as the ratio of the observed deflection amplitude in the presence of scattering to the amplitude of the deflection in the absence of scattering. So the total deflection of the probe beam is proportional to an excitation beam power and the clarity factor can be calculated simply using relation (2.31) which is described by Spear in 1990 as:

$$C.F = \frac{\int_0^Z P_0 \exp(-\alpha_s z)\, dz}{\int_0^Z P_0\, dz} = \frac{(1 - \exp(-\alpha_s z)}{\alpha_s z} \qquad (2.33)$$

Where P_o denotes the available power incident on the sample at z = 0.

This expression which is given by equation (31) is valid only for collinear PTLD systems, and it represents the attenuation in the mirage signal that is due to scattering. Therefore, if the PTLD signal is used to evaluate α_a for a sample of known measurable α_s, at the excitation beam wavelength, the measured value must be adjusted by this factor (Spear et al, 1990).

2.6 Detection of light deflection

2.6.1 Position sensor:

Various kinds of position sensors were used to detect the position of light beam reflected from a specific target. Some sensor measurements are geometry includes a collimated emitter source, as laser diode, and position sensitive detector (PSD) where the position of the reflected beam depends on the target distance and distance from source (Massari, 2002).

Some detectors are used to measure the position of a light spot in one and two dimensions such as PSD which is discovered by Schottky in 1930. 1-D PSD is used to measure a linear displacement. When a target that light beam is projected on is moved a distance

Δd_0, and by knowing the reflected angle ø from the target so the displacement is given as:

$$\Delta d_0 = \frac{\Delta d_1}{2 \cos \phi}$$

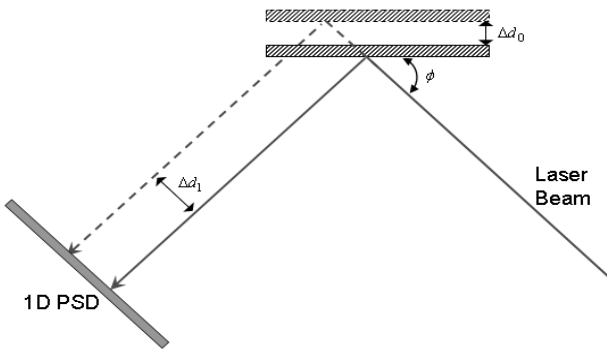

Fig.2.5: Displacement of the reflected beam measured by a PSD.

Another common application of PSDs is to measure rotation about a fixed point by the following equation.

$$\frac{\phi}{2} = tan^{-1}\left(\frac{2\Delta d}{L}\right)$$

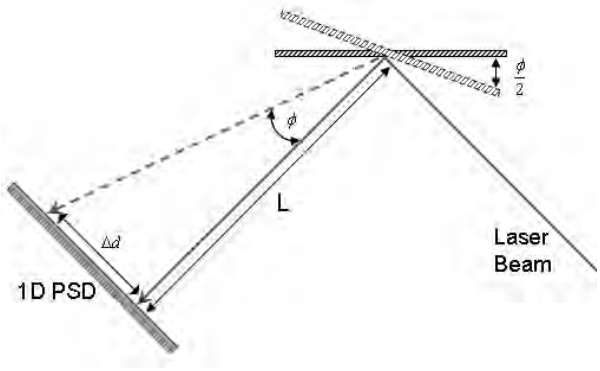

Fig.2.6: Measurement principle of rotation around a fixed point by a PSD (Afte: Henrik, 2008).

PSDs converted the light incident into electrical current (Henrik, 2008).

Aculux sensor, is an example of 2-D optical position sensor, it contains high accuracy lateral effect photodiode to produce four photo currents proportional to light spot intensity. This sensor reads the result as digital as the position sensor in Figure 2.7.

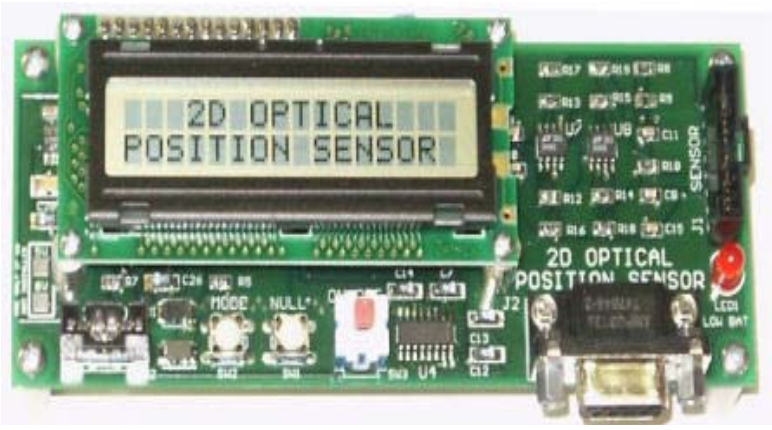

Fig. 2.7: Photo of 2-D optical position sensor (after: Aculux, LLC)

2.6.2 Light diffraction method:

When a light of certain wavelength is passing through slits, there will be bright and dark spots formed on far screen, i.e. diffraction pattern. According to Huygens' Principle, each portion of the slit acts as a source of waves. Hence, the two lights from the portions of the slit can interfere.

A central peak containing most of the light intensity accompanied by secondary higher-order maxima and intensity minima governed according to (destructive interference):

$$sin\ (\theta) = m\lambda\ /d \tag{2.34}$$

The first dark fringe occurs at the angles given by equation 35:

$$sin\ (\theta) = \lambda\ /d \tag{2.35}$$

where θ is the angle between the central incident propagation direction and the first minimum of the diffraction pattern, and *m* indicates the sequential number of the higher-order maxima. Usually, interest is in the location of the first minimum, when m = 1, because most of the light energy is located in the central diffraction maximum. Light intensity is maximum at θ = zero degrees, and decreases to a minimum at angles dictated by the equation above.

There are two secondary maxima bounded on both sides of a central brightness maximum, the intensity of each succeeding secondary maximum decreasing as the distance from the

center increases as in Figure 2.8 which illustrates the beam intensity versus diffraction radius (Halliday and Resnick, 1981).

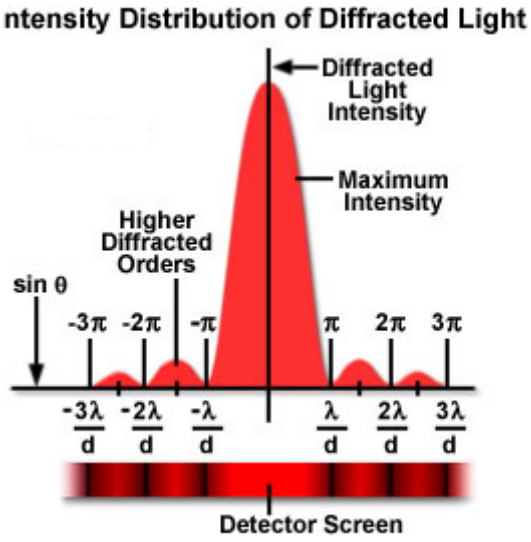

Fig.2.8: Intensity distribution of diffracted light

(After: http://micro.magnet.fsu.edu/primer/java/diffraction/basicdiffraction, December2008).

When the wave arrives at the single slit as a plane wave, single slit diffraction pattern has a central maximum that covers the region at m=1 dark spots. The first secondary maximum appears between the m=1 and m=2 minima (not exactly half). The secondary maximum has a weaker intensity than the central maximum. The resulting relative intensity will depend upon the total phase displacement according to the relationship (Young, 1992):

$$I = I_0 \frac{\sin^2\left[\frac{\delta}{2}\right]}{\left[\frac{\delta}{2}\right]^2} \tag{2.36}$$

This total phase angle can be related to the deviation angle θ by:

$$\delta = \frac{2\pi\, a \sin\theta}{\lambda} \tag{2.37}$$

The intensity as a function of angle θ is given (Young, 1992) by:

$$I = I_0 \frac{\sin^2\left[\frac{\pi\, a.\, \sin\theta}{\lambda}\right]}{\left[\frac{\pi\, a \sin\theta}{\lambda}\right]^2} \tag{2.38}$$

In the present work the diffraction pattern is initiated with a helium- neon laser. The above diffraction idea, i.e. when the beam position is changed by certain angle it is followed by a change in the reading of a photometer (intensity). This technique is suggested by (Abu-Taha, 2008) in the present work to replace the normal position sensor in determining any minute shifts of the light beam.

Chapter Three

Experimental set up

3.1 Introduction

In this chapter a general view and a schematic diagram of the complete experimental setup are described and shown in Figures 3.1 and 3.2 respectively. The experimental equipment constituting the advancement of technology, especially in data collection allows easy to handle process, data collection, and stage analysis is all made simple and efficient. Results are simultaneously recorded using two methods CLD technique and PTLD technique. A detailed description and the physical operating principles of both systems components are given and taken for known samples used to authenticate the systems, results for unknown samples are then taken by using the two techniques, and their results compared.

3.2 Equipment used for both experiments

The equipment used in this study including the two different glass boxes which will be described in sections 3.3 and 3.4, single slit (0.6 mm wide) that is used to produce a diffraction pattern of the reflected probe beam upon leaving the gas directly, a photometer which records the light intensity value, power function generator, connecting leads, ordinary reflecting mirror fixed on the internal box wall, He-Ne laser beam is used as a probe beam, IR radiation is obtained from a miniature pulsed wideband IR source as discussed in section 3.5. The source is driven by an AC signal form a power function generator, a current of 0.2 Amps is needed to drive the source. Radiation is allowed to fall above certain amount of sample placed in the bottom of glass box, the radiation hence passes through sample gas emissions. An absorbed radiation generates a shifted (right or left) principle maximum spot that is projected on a photometer's head, this shift was a result of refractive index gradient and it could be detected by taking the change in light intensity recorded by a photometer.

3.3 Conventional light deflection experimental system.

In the present study two different cells were used. The first cell used to study the effect of different trace gases of different samples on the path of light beam which is deflected by the effect of induced refractive index, i.e. ordinary refractive index gradient. CLD cell consisted of a piece of mirror fixed on the internal box side. The box dimensions were 5 cm × 5 cm × 4.5 cm.

The sample to be studied was determined and maintained in the bottom of box using a micro peptide if it is a liquid sample (for example: methanol and acetone) and other samples weighed by an impressible balance. Then a probe beam of a He-Ne laser was allowed to pass over samples so as to be in the way of the rising up gas emissions. The reflected beam from the mirror glued on the opposite side of the box is allowed to pass through a slit such that the produced 1^{st} order maxima fall on the window of the photometer head. It is very important that the reflected beam is in the same plane of the incident beam otherwise the principle maxima will be shifted at an angle making measurements very difficult. The resulting diffraction pattern is used to assign beam deflection. The center of the principle maximum spot must be allowed to fall on the head of a photometer prior to the introduction of sample in the cell, then any index change in the box due to change in sample condition will result in maximum shift allowing to measure light deflection, i.e. beam position change.

A general schematic diagram of the experimental setup of convention light deflection spectroscopy suggested here is shown in Figure 3.1.

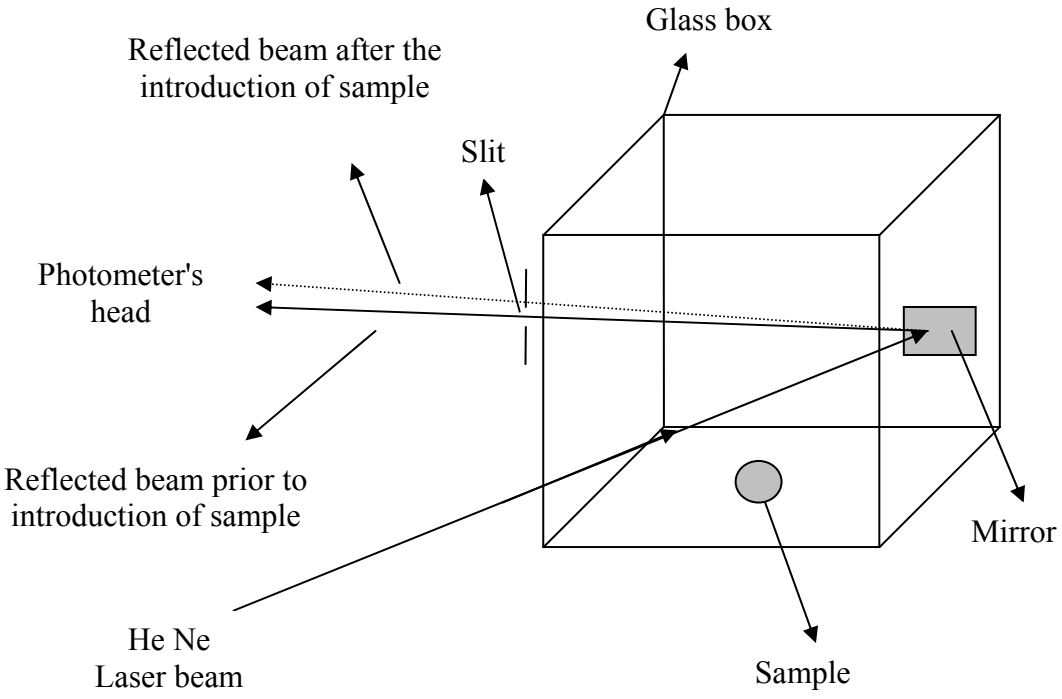

Fig.3.1a: Schematic showing the conventional Light Deflection in the cell used to detect gas trace emissions from different samples.

Fig.3.1b: Photo showing the complete conventional light deflection Experimental set up used to detect gas trace emissions from different samples.

3.4 Photothermal light deflection experimental system.

PTLD cell was the same cell used for CLD experiment as described in section 3.3, but an infrared radiation source connected with a function generator were added to the cell in the case of PTLD measurements. The present experiment was carried out to study the effect of thermal gas absorption infrared radiation compared with the results of CLD method.

An infrared (IR) source used to emit thermal radiation requires to excite samples. It is fixed on one of the glass box's sides so that its radiation passes through sample gas emission. So gas emission from samples can absorb thermal radiation and the result would be a refractive index gradient which affected the path of reflected beam before it falls on the photometer's head. The effect of the IR absorption observed as a shift in position of the principle maximum spot that coincides with photometer's head before absorption takes place. The IR source was powered by a power function generator at 10 Hz frequency, and 5volts. A general schematic diagram of the experimental setup for Photothermal Light Deflection set up is shown in Figure 3.2.

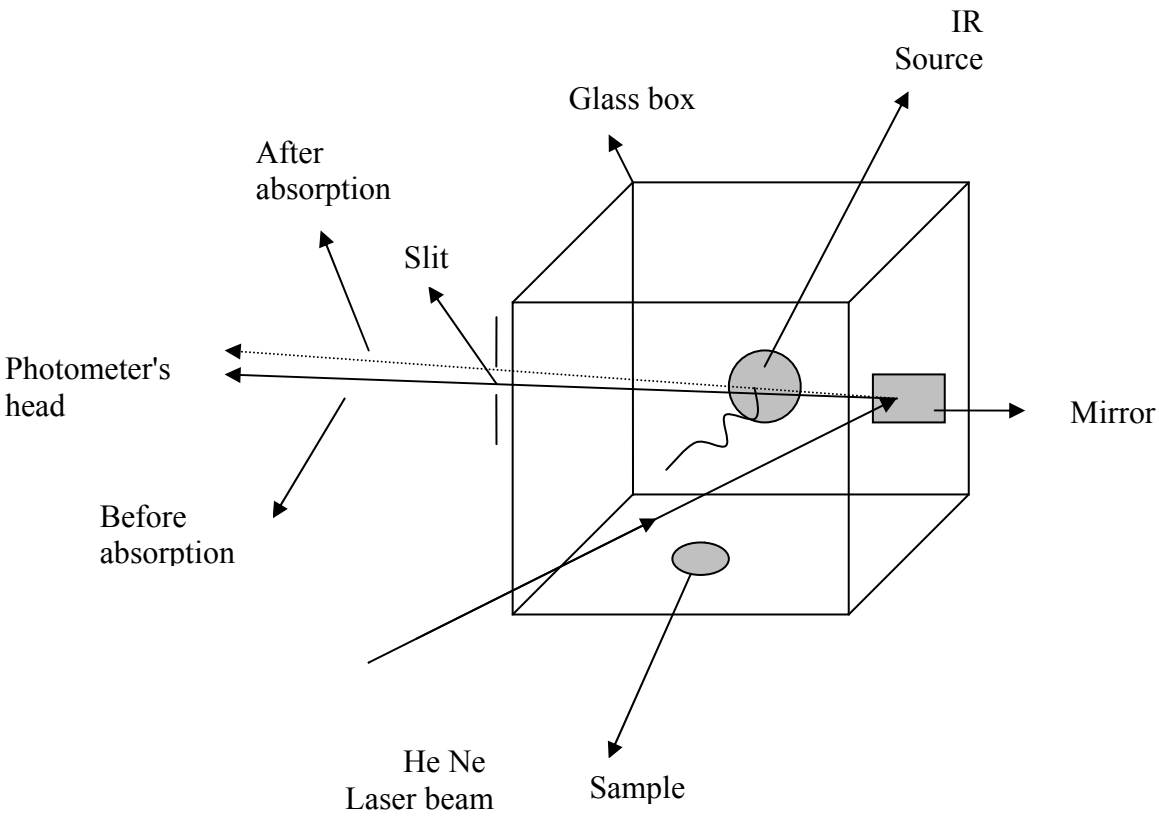

Fig.3.2a: Schematic showing the PTLD experimental setup used to detect trace gas IR absorptions.

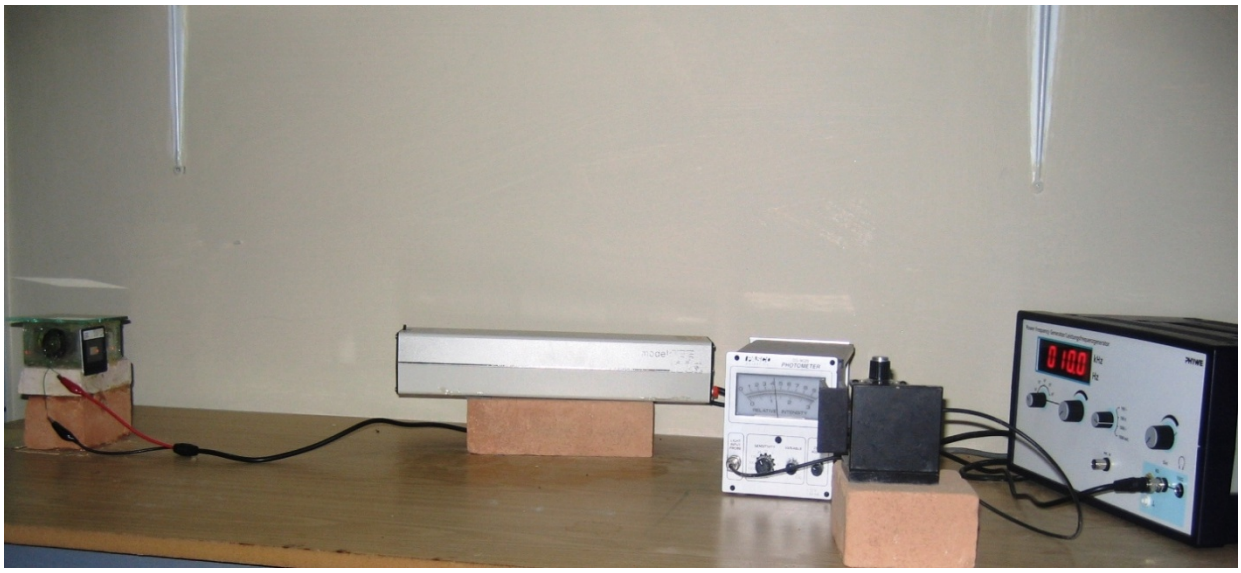

Fig.3.2b: Photo of the PTLD experimental setup used to detect trace gas IR absorptions.

3.5 Wideband infrared (IR) Source.

The infrared source used in this study is a wideband pulsed mid-IR thermal source based on electrical heating of a thin metal alloy foil up to heat (~900°C) and cooled by its own radiation. The device, with emitting area diameters ranging from 25 mm to 1.7 mm, is based on a suspended bispiral metal foil geometry which offers substantial thermal isolation from the supporting structure. The infrared emission is two sided, but the reverse side radiation may be reflected through the plane of the bispiral heater to enhance the total forward emission. Practical devices are described in respect of their mechanical, electrical and infrared emitting properties. An encapsulated form of the smallest device incorporates an infrared transmitting window and infrared beam directivity and intensity-enhancing focusing reflector, and has a typical modulation depth of 85% at 10 Hz. (Laine, 1997)

3.6 The photometer

The photometer is used to detect intensity change in the reflected beam, which is translated as a change in position. Pasco model OS-8020 photometer is used in the present study to detect the polarized light. This photometer can measure light level down to a sensitivity of 0.1lux (the level of illuminance on a night with a full moon). The light intensity level, from the polarized beam in a darkened room, is in the range of 0.1-3 lux, and dependent on the wavelength of the light.
(http://www.fceia.unr.edu.ar/fisicaexperimentalIV/Pasco/High%20sensitivity%20photometer, December 2008)

Fig 3.3: Photo for the Pasco OS-8020 Photometer and its head

The photometer head could be mounted, on a stand, as the rightmost component on the optical rail, and the opening in the fiber is placed directly along the beam path. Next, slowly move the optical fiber to let the center of the principle maximum light spot fell on it. This may cause the focused light beam to exceed the entrance diameter of the fiber cable. This is acceptable since there is a need to get as much light into the fiber as possible. Similarly, the brightness of the focused spot can be simultaneously monitored on the Pasco meter display and signal proportional to light intensity can be obtained its analog- meter.

Photometer adjustment: The analog meter connected to the optics cable needs to be properly adjusted in order to obtain reliable results. To do this, a piece of paper is placed in front of the optics cable, to block the colored light beam. Now, the zero offset is adjusted, so that the meter reading is nearly zero. Next, the sensitivity on the meter is adjusted so that the needle deflects to nearly full scale. For this, the gain on the meter may also need to be adjusted. The piece of paper is removed from the beam path. The meter reading should now be roughly stable and fluctuations of one or two small divisions may be observed.

3.7 Detection scheme:

In photothermal deflection spectroscopy it is custom to use a position sensor to detect the level of deflection in the reflected beam after passing through the trace gas emissions resulting from introducing the sample into the glass box. Sensitive position sensors are expensive and very delicate and tricky to use. In the present study a new technique was suggested for the first time (Abu-Taha, 2008) to allow accurate measurement of deflection in both methods. It includes the introduction of a slit, so that the emerging beam from the slit will form a diffraction pattern and any deflection either ways will show itself as a change in the intensity of the parts of the principle maxima, hence a change in the voltage signal of the analog meter of the photometer allowing to detect any minute changes due to direct index change as that due to absorptions by gas molecules to the power from the pump beam. Full details and theoretical coverage are discussed in section 2.6.2.

3.8 Experimental setup and procedure.

Equipment are arranged such that conventional light and the photothermal deflection processes had the same setup for all parts of the experiment. At first and before taking any results, CLD experiment was arranged as in Figure 3.1a, laser switched on and its beam is allowed to inter the glass box. The reflected beam passes through the single slit. Photometer's head is adjusted (see section3.6) that it’s head is sensing the principle maximum spot, then manually the head is moved to measure light intensity change versus the distance as maximum is scanned away from a center of first maximum spot. This is a trial carried out to confirm the sensitivity of our system and make sure that data will result in a diagram similar to that of the diffraction pattern as shown in Figure 3.4.

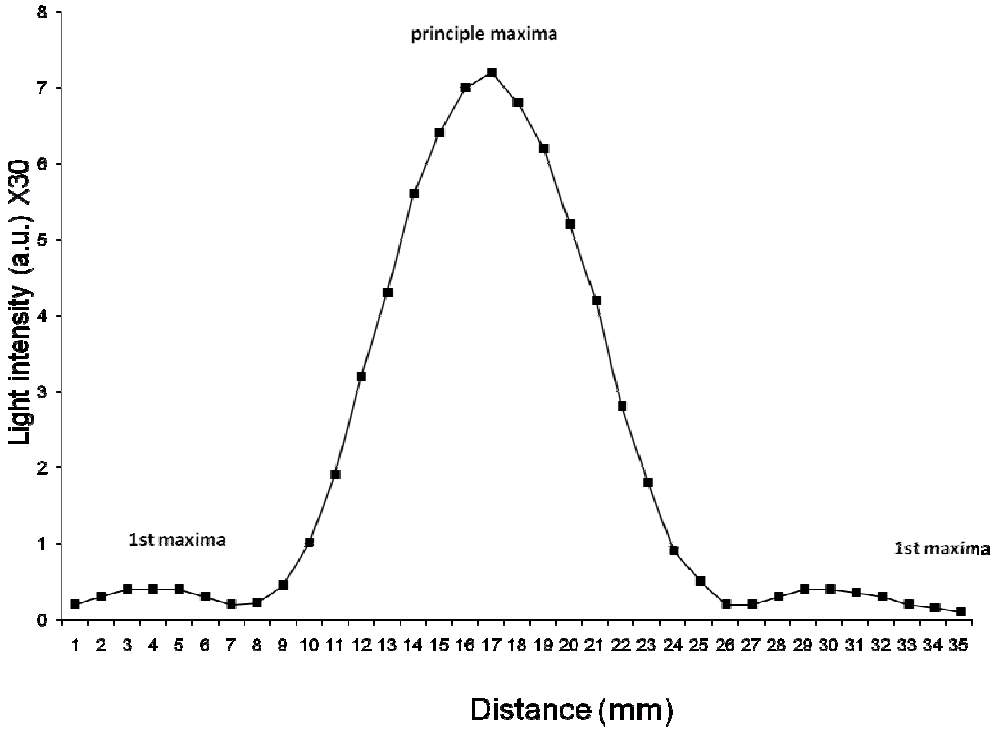

Fig.3.4: The relation between light intensity in (a.u.) and distance in (mm) from a center of the principle maxima.

The smallest reading by the photometer = 0.1 Lux. when the light beam deflected was moved o.5 mm the photometer reads

$\frac{6}{0.1}$ = 60 *Units* 2×30 = 6 lux the smallest number of unit in 6 Lux =

0.5mm ⟶ 60 units

1mm ⟶ $\frac{60\times 1}{0.5}$ = 120 units

So the smallest scale reading by photometer equals 1/ 120 of mm, this means that when the beam shifts 0.0083 mm the reading of the photometer change to its smallest scale.

3.9 Experimental samples

Two different samples of known structure and three unknowns were used in this study.
The known samples were properly chemicals materials for example; a Methanol CH3OH and acetone (CH3)2CO. Other used samples were leaves, Seeds and flowers; their trace gases are being detected, although not known. Two different samples of each type were used. Each sample was studied by the two methods. i.e. employing the two different techniques.

3.9.1 Standard samples:

Methanol and acetone were used as known samples, to detect their gas emissions by both methods. Three different methanol volumes were used in both CLD and PTLD methods, three different acetone volumes were used CLD method and two in PTLD method, since when 20µl of acetone were used it was evaporated very fast (the evaporation time couldn't be taken). These two were picked up from university lab.

Methanol is the simplest alcohol, and is light, volatile, colourless, flammable, poisonous liquid with a distinctive odor. At room temperature it is a polar liquid and is used as an antifreeze, solvent, fuel, and as a denaturant for ethanol, the refractive index of methanol is 1.325 (http://en.wikipedia.org/wiki/Methanol, December, 2008).
Acetone $(CH_3)_2CO$ is the simplest example of the ketones. Acetone is miscible with water, ethanol, ether, etc., and it could be found in our homes; it is used to remove a nail polish and as paint thinner, it produced from propane directly or indirectly. The acetone's refractive index is 1.355 (http://en.wikipedia.org/wiki/Acetone, December, 2008).

3.9.2 Unknown samples:

Three different sample types; seeds, flowers and leaves, of unknown gas species were used in both CLD and PTLD methods. Fresh leaves and flowers were taken from the garden in the same day of these samples investigation. Each of these samples emit specific kinds of gases, so when they are placed inside the box the concentration of gases will be increased inside the box, that effected the refractive index which in turn affect the passage path of the reflected beam. Each samples of known and unknown gas structure was placed in the box in a region so that IR radiation passes through its gas emission.

3.10 Authentication of the experimental system.

A set of known samples was used to examine the authenticity of experimental setup to gain enough knowledge and experience and confirm the system reliability. Both of the two parts of experimental arrangement were investigated using standard methanol and acetone samples as small as 20 μL, 40 μL and 60μL. Different signals from different samples were obtained. The CLD and the PTLD signals were simultaneously detected and compared. Following the same way, other samples were investigated.

3.11 Conclusion

Two detection systems schemes were designed to detect trace gases of different samples. These systems were assembled and examined using known samples. The compared results of the two experimental parts show the effect of the absorption on the signal, and prove which of the two arrangements are more sensitive. For further understanding and authenticating of the results, many samples can be studied using the two techniques and compare the results.

Chapter four

Results

4.1 Introduction

In this chapter the experimental results are introduced. The CLD and PTLD signals have been studied using different types of samples. The results of the known samples were discussed in view of the obtained data by using the two experimental techniques. The same was done with the other samples i.e. the unknown samples. Comparison between the results of the two techniques for each sample were compared and discussed. In the view that one of the techniques, namely CLD method could be identified as a new simple, less expensive, easy to use than the PTLD. Results are presented, analyzed, and discussed in sets as they are introduced in the following sections. Comments will be pointed individually for each experiment and totally as collective results of the experiments. Finally the result of using these two techniques in open air and open room will be discussed.

4.2 Authentication of results

To test the authenticity of results, i.e. that the signal produced by the sample is free from other environmental effects surrounding the system, experimental set up is arranged in its normal way, probe beam from He-Ne laser is allowed to pass and diffraction pattern is formed, signal was then monitored for at least half an hour to make sure that the signal stays stable, i.e. no other effects in the vicinity of the system can introduce any change in the assumed effect.

4.3 Standard sample results

Using both experimental set up of this study, Methanol CH_3OH and Acetone $(CH_3)_2CO$ vapors are used as known materials to investigate the system reliability. At the beginning of each part of the study three different volumes of Methanol and Acetone (20, 40 and 60 μL) were used to test the system ability to detect trace gases, plants tissue and to ensure the detection ability of the newly designed system.

4.3.1: Intensity versus time signal

In this study gas traces would be detected by both techniques, i.e. CLD and PTLD. Signals levels are dependant on the concentration of trace gases that could be released from the sample. Different samples with different gaseous emission were used. By increasing the volume of the added sample, it is expected that signal saturation could be reached. For each sample increment, the known volumes were placed in the box and it is closed immediately. Signal is recorded against time for nearly 90 minutes for CLD technique and 60 minutes for (PTLD) technique.

The readings of the light intensity were taken by using a photometer, light incident on a single slit after it was reflected from the mirror fixed on box's wall front of single slit's wall as shown in Figure 3.1. When a reflected beam passed through the single slit, forming diffraction pattern as shown in Figure 2.8. The center of the principle maxima spot was made to coincide with the fixed photometer's fiber optic head. So at the beginning the reading would be maximum intensity, and by time intensity reading would be decreased as the beam deflection increased since the principle max-spot would shift by the refractive index gradient which caused a gradient index in the way of the deflected light.

For each sample the reading of the intensity difference were taken versus time.

4.3.2: Methanol results.

Methanol is a volatile material that causes a gas trace which could be detected by using CLD and PTLD effect. Three different volumes of methanol (20, 40 and 60 µl) were used. Figure 4.1a shows the decrease in light intensity due to the increase of methanol evaporated molecules of different volumes used in the CLD technique. Figure 4.1b shows the intensity decrease due to the increase of methanol evaporated molecules of different volumes used in the PTLD technique and Figure 4.12 shows the comparison between 40 µL methanol CLD's result and 40 µL methanol PTLD's result which show the absorption effect.

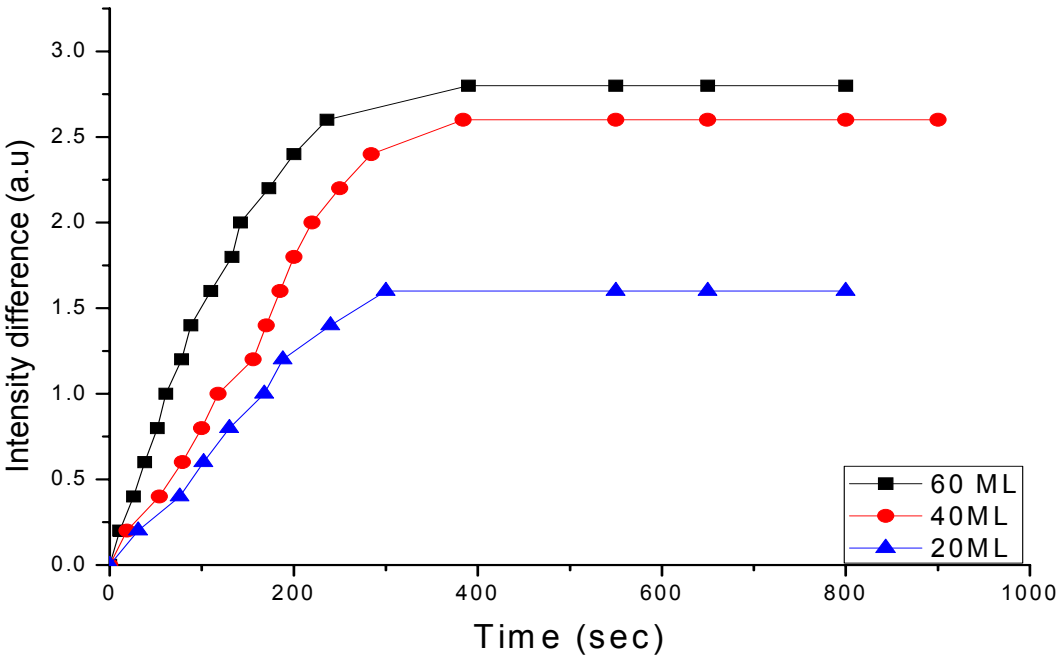

Fig.4.1a: Monitoring gas trace emissions of three different Methanol's volumes using CLD technique.

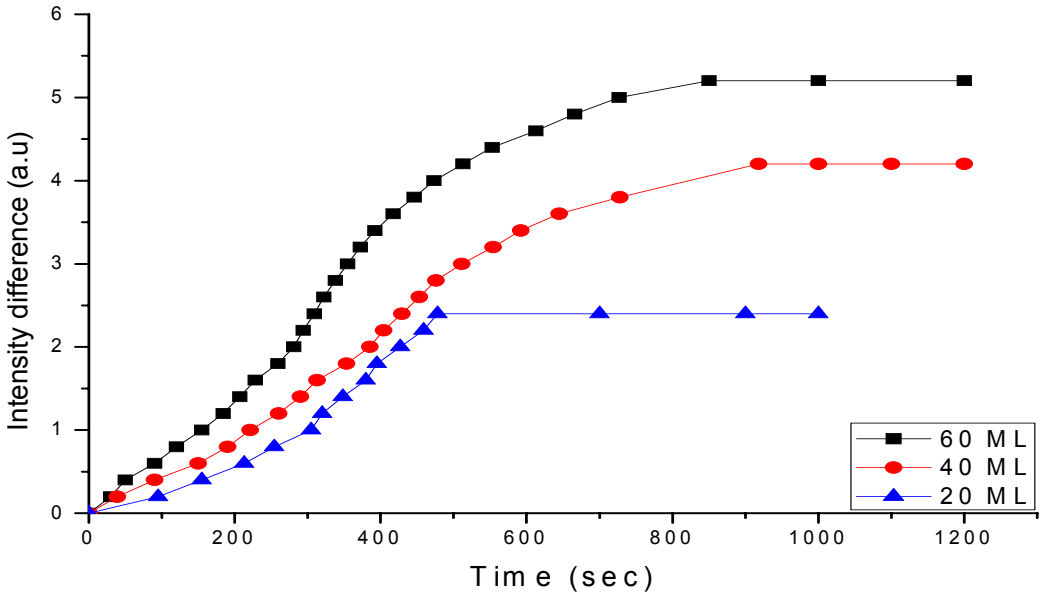

Fig.4.1b: Monitoring gas trace emissions of three different Methanol's volumes using PTLD technique.

4.3.3: Acetone results

Acetone is a volatile material that causes a gas trace which could be detected by using CLD and PTLD effect. Three different Acetone volumes of (20, 40 and 60µl) were used. Figure 4.2a shows the decrease in the intensity due to the increase of the amount of evaporated Acetone molecules of the different volumes using CLD technique. Figure 4.2.b shows the intensity decrease due to the increase of Acetone evaporated molecules of different volume using PTLD technique.

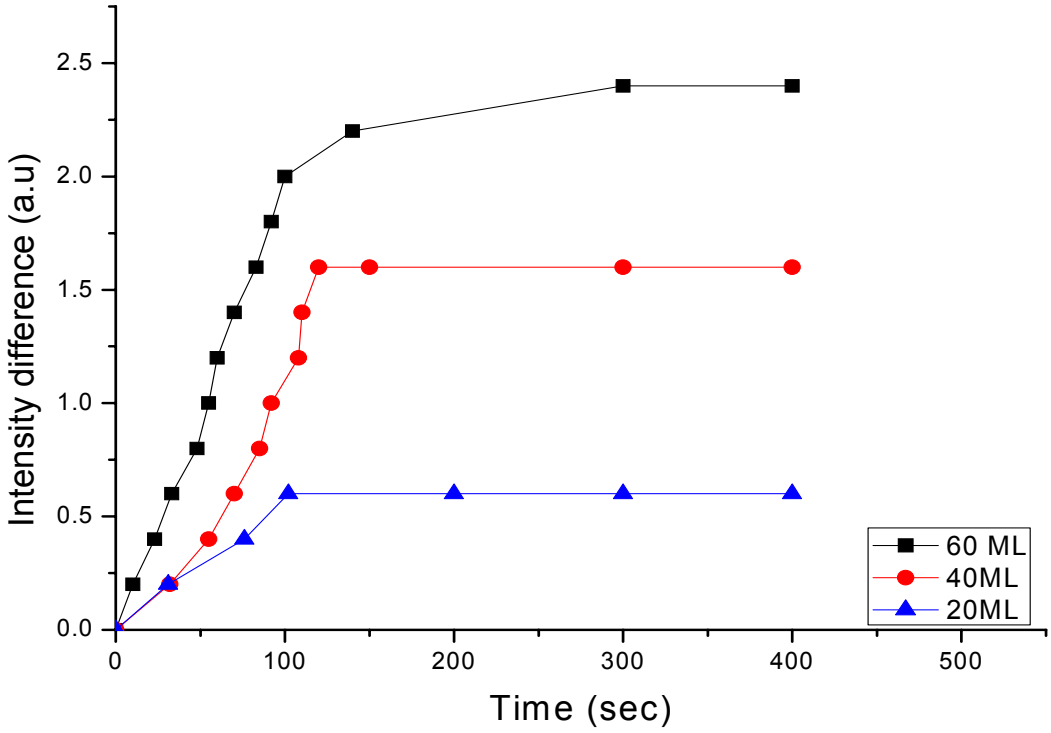

Fig.4.2a: Monitoring gas trace emissions from different Acetone's volumes using CLD effect technique.

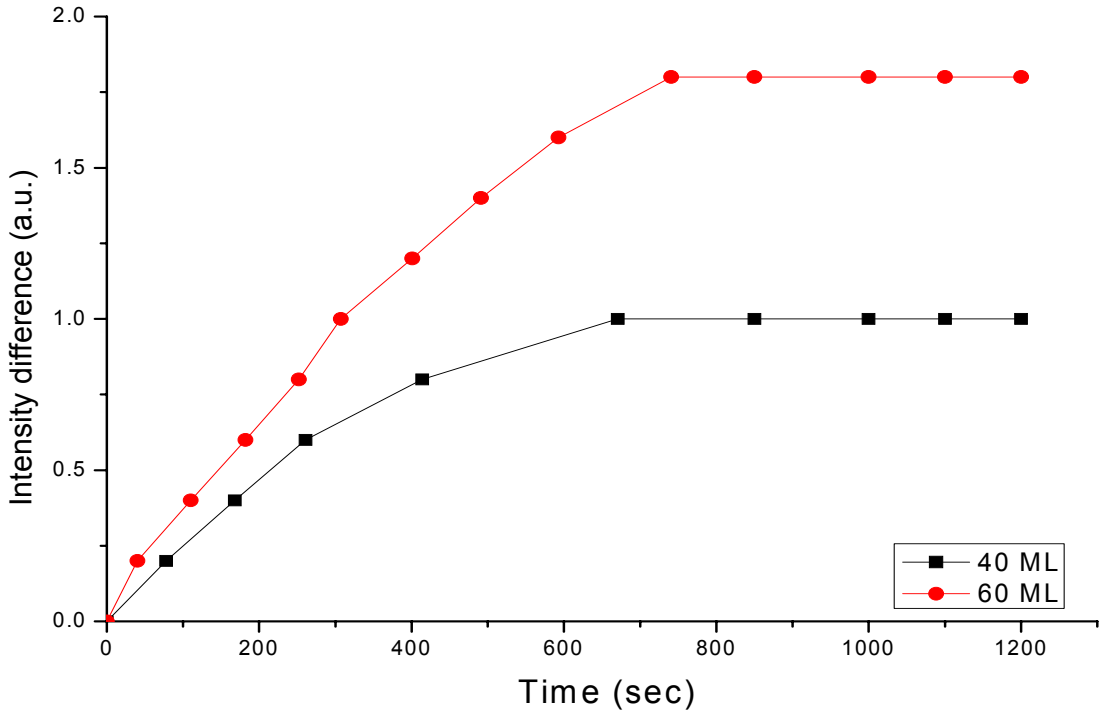

Fig.4.2b: Monitoring gas trace emissions from different Acetone's volumes using PTLD effect technique.

4.4 Unknown samples test.

Three different samples (seeds, flowers and leaves) were allowed to emit gases that are investigated by the simultaneous CLD and PTLD techniques using the system shown in Figure 3.1 and in Figure 3.2. The corresponding experimental results are shown in the following sections.

4.4.1 Leaves results (mint and sage):

Two different masses of mint and sage were used to study their gas traces by CLD and PTLD techniques.

Fresh plants leaves namely mint and sage were taken from the garden in the same day of investigation. Definite masses of the two plants were used (0.25g and 0.50g) respectively. The gas emission from these plant's leaves is a mixture of gases among which is water vapor, that has its refractive index effect on the light beam traversing the region above the sample. Concentration and the speed of gas emission could be increased by crushing the leaves.

Figures 4.3a and 4.3b show the CLD mint's results. Figure 4.3a shows the effect of different masses on trace gas emission used 0.5g and 0.25g of uncrushed mint. Figure 4.3b shows the difference between the levels of gas emission from 0.5g crushed mint and 0.5 g of uncrushed mint's leaves. Figure 4.4a and Figure 4.4b show the PTLD mint's results. The same were done for sage, using two different masses (0.50g and 0.25g); sage's leaves were crushed to increase the speed and concentration of sage's gas emission. Figures 4.5a and 4.5b show the CLD sage's results.

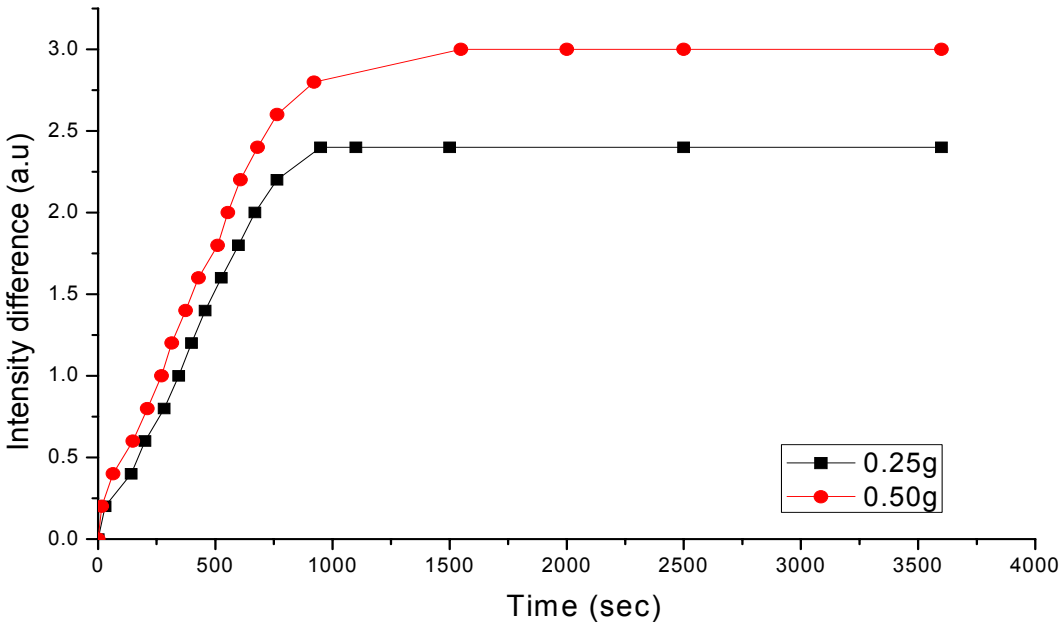

Fig4.3a: Monitoring gas emissions from two different crushed mint's masses using laser CLD technique.

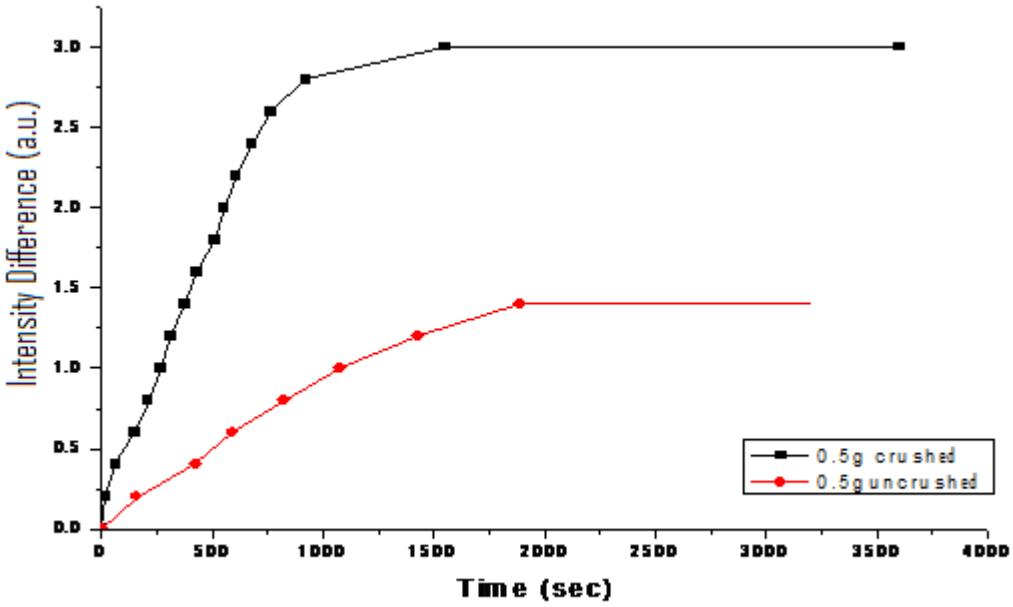

Fig 4.3b: Comparison between gas emissions from 0.5 g crushed and uncrushed mint's leaves (rate of gas emission) using laser CLD technique.

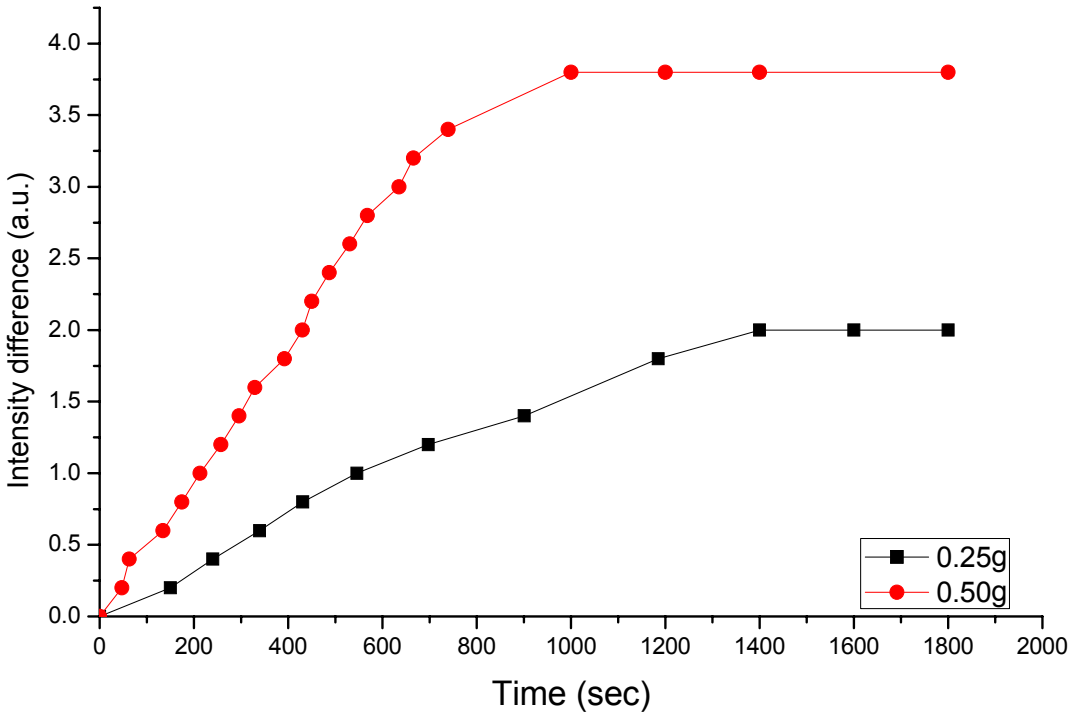

Fig 4.4a: Monitoring gas emissions from two different crushed mint's masses using laser PTLD technique.

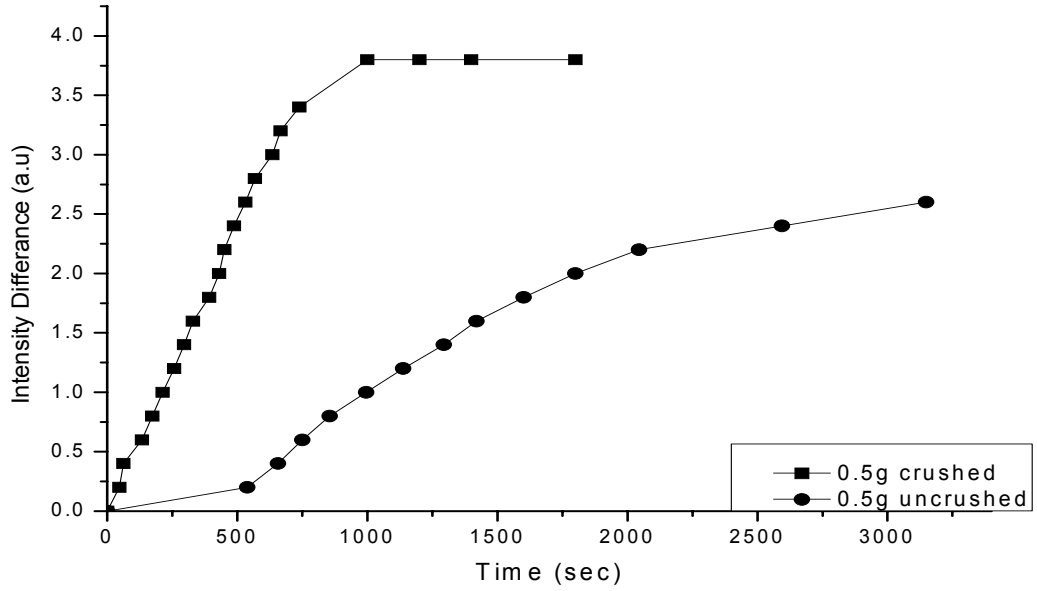

Fig 4.4b: Comparison between gas emissions from 0.5 g crushed and uncrushed mint's leaves (rate of gas emission) using laser PTLD technique.

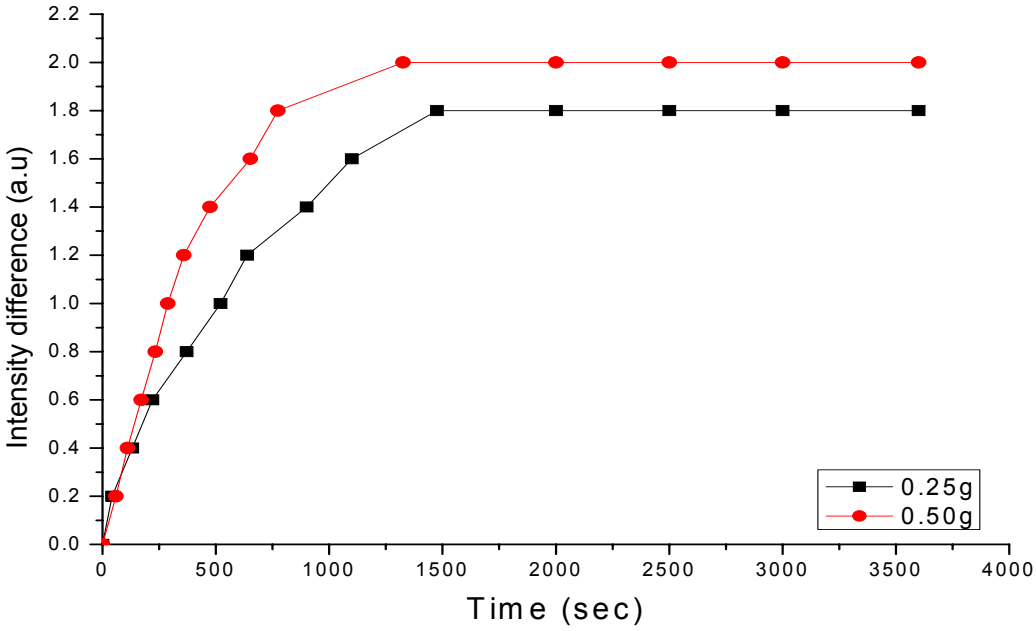

Fig 4.5a: Monitoring gas emissions from two different crushed sage's masses using laser CLD technique.

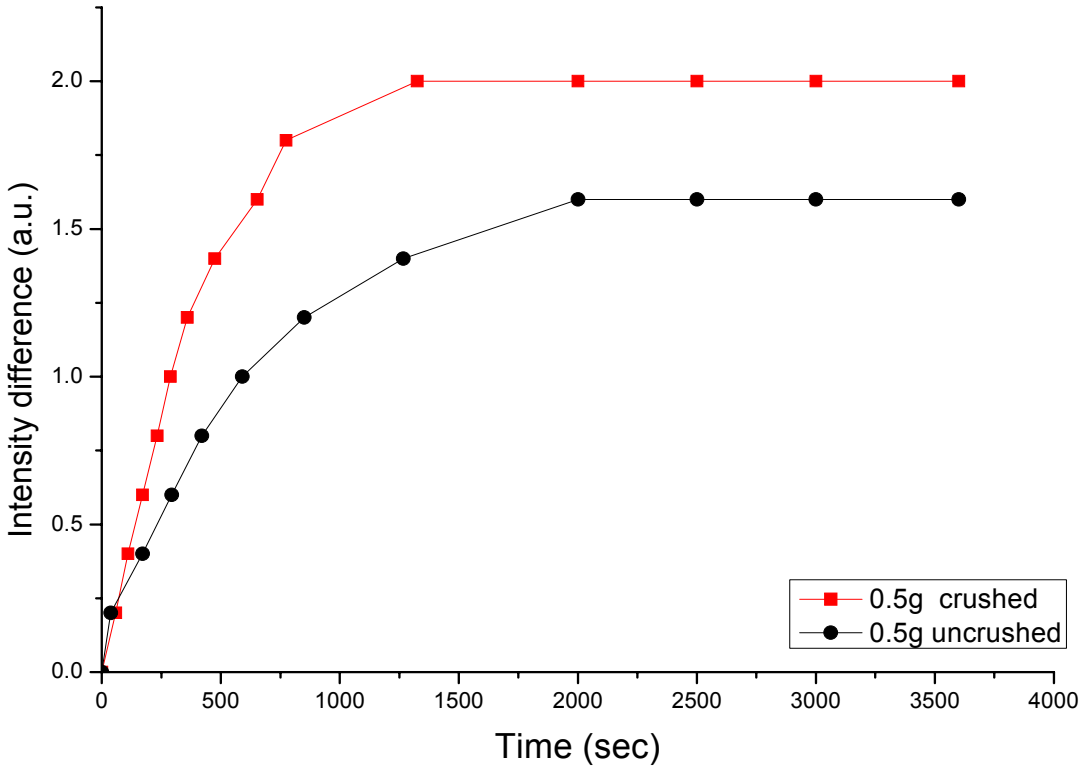

Fig 4.5b: Comparison between gas emissions from 0.5 g crushed and uncrushed sage's leaves (rate of gas emission) using laser CLD technique.

4.4.2 Results for Flowers (Jasmine and Rose):

Two deferent kinds of flowers (Jasmine and Rose) were investigated using CLD and PTLD techniques. For each flower type two flower colors were used. Procedure followed for mint and sage were followed for the case of jasmine and rose.

In the case of Jasmine flower the plant of Jasmine has two different colors in itself, white and yellow. By using these two new techniques CLD and PTLD an investigation of the level of emission associated with each color is carried out. Figure 4.6a shows a comparison between white and yellow Jasmine's flower gas traces (the effect of Jasmine's

color). Figure 4.6b detects the effect of gas emission speed and concentration on the deflected laser beam. Figures 4.6a and 4.6b show the results of CLD technique and Figure 4.7 show a comparison between Jasmine's white and yellow trace gas emission using PTLD technique, the effect of Jasmine's flower color on the level of emission.

White and red Rose flower were used in Figure 4.8a, a comparison between white and red Rose's gas trace. Figure 4.8b shows the effect of gas emission speed and concentration on the level of laser beam deflection. Gas's emission speed and concentration were increased by crushing the flowers. Figures 4.8a and 4.8b were the results for CLD technique.

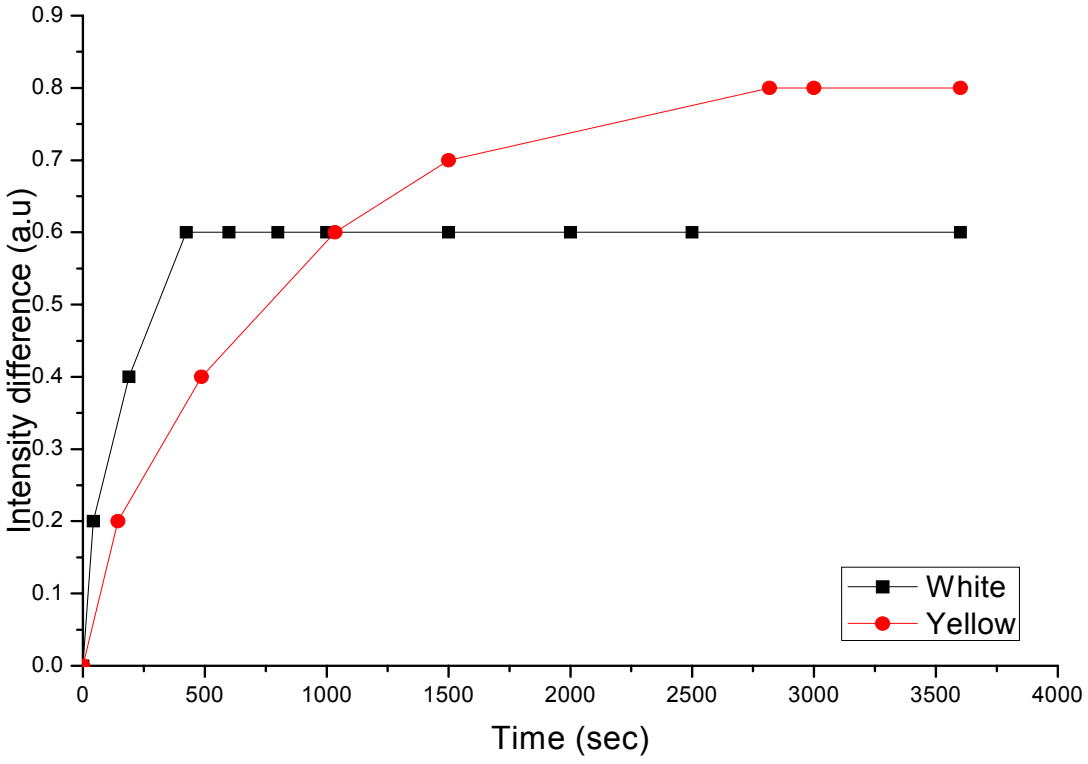

Fig 4.6a: Comparison between white and yellow Jasmine flowers trace gas emissions using CLD technique.

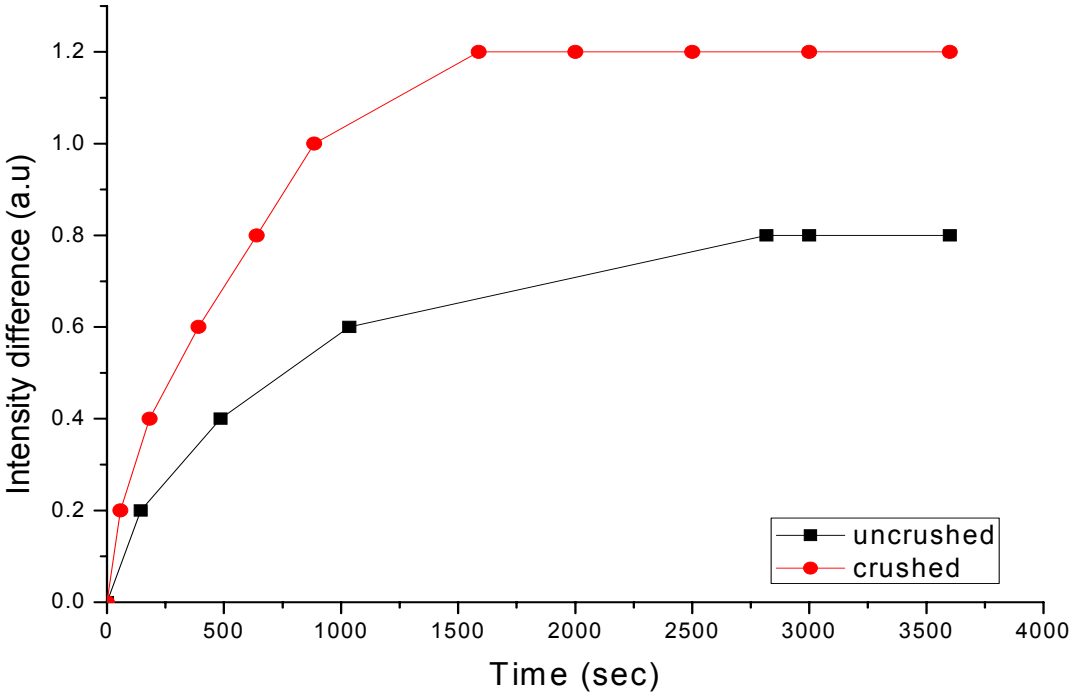

Fig 4.6b: Comparison between crushed and uncrushed yellow Jasmine flowers trace gas emissions using CLD technique.

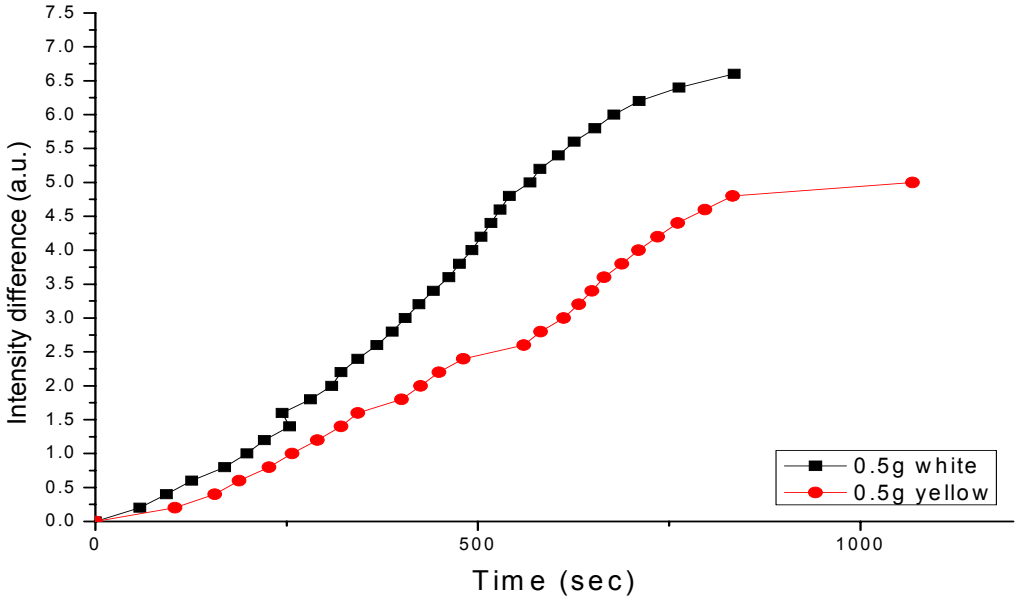

Fig 4.7: Comparison between white and yellow Jasmine flowers trace gas emissions using PTLD technique.

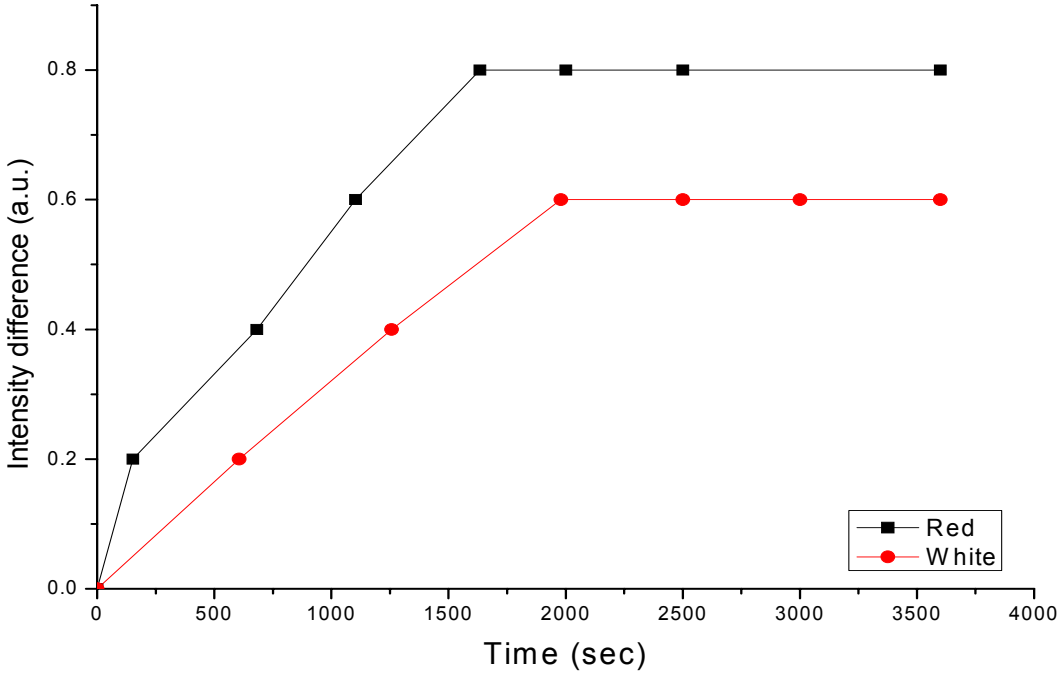

Fig 4.8a: Comparison between white and red rose flowers trace gas emissions using CLD technique.

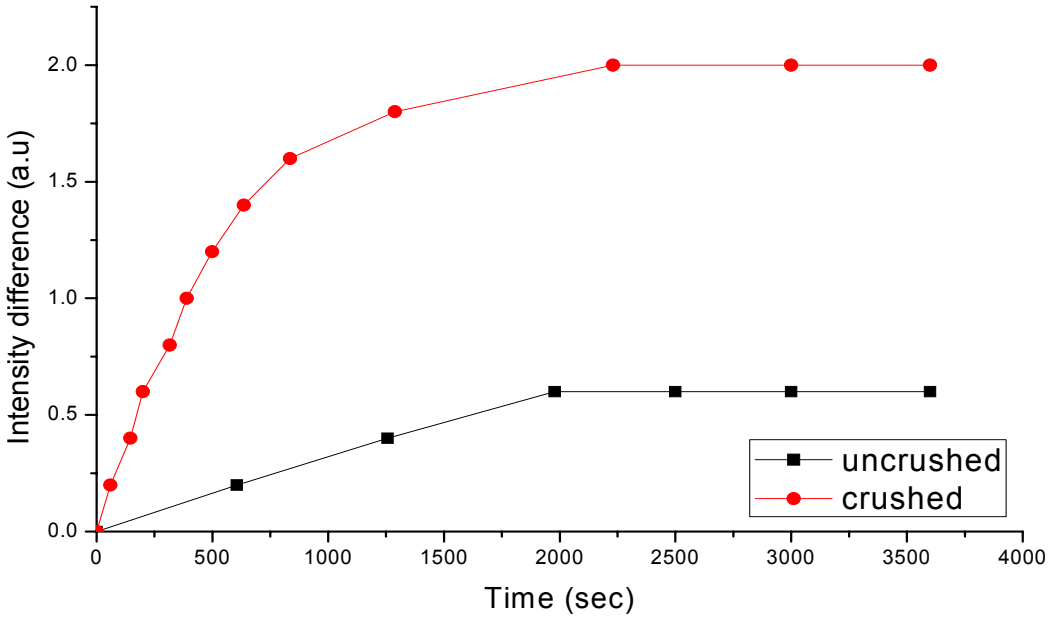

Fig 4.8b: Comparison between crushed and uncrushed white rose flowers trace gas emissions (rate of gas emission) using CLD technique.

4.4.3: Results for seeds (Wheat and Chick peas)

Two different masses of seeds namely wheat and chick peas were investigated using CLD and PTLD techniques. It's known that chick peas can be attacked by caries insects. The present study was employed to confirm the ability of the system to check for insect actions in seeds specially while they are in stores, this is done by detecting their gas emissions when insect contain infected seeds were introduced in the testing box. Figure 4.9 shows a comparison between healthy and contaminated chick peas using CLD technique, and Figure 4.10 shows a comparison between healthy and contaminated chick peas using PTLD technique.

In the case of wheat, comparison was sought between germinated and un germinated seeds. To have a germinated wheat grains they were placed in wet cotton for three days until it began to germinate, but their germination still could not be seen by the eye, i.e. the idea is to predict germination before it is clear to the observer. Two grams ≈ 44 grains of germinated wheat were taken and placed, results are shown in Figure 4.11.

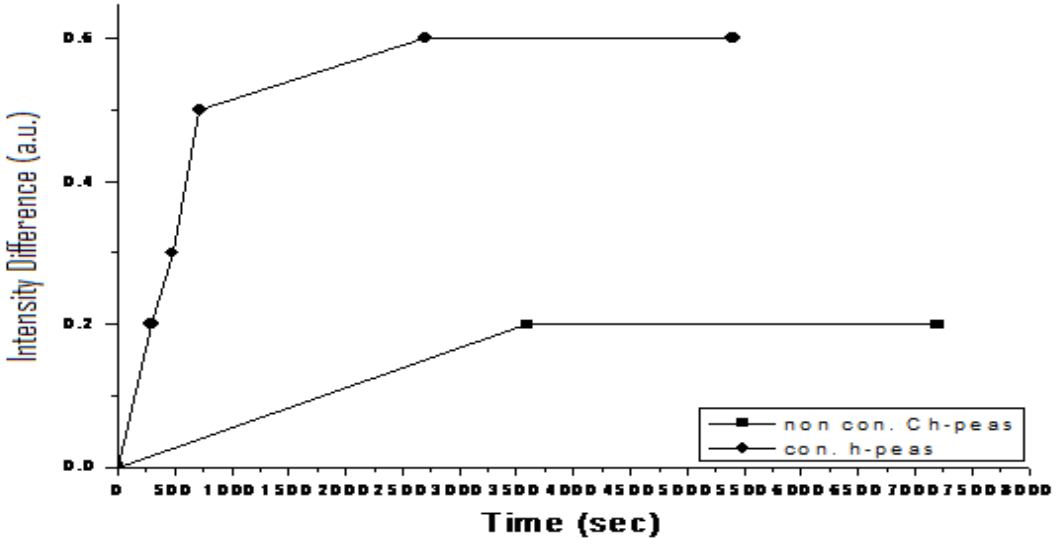

Fig 4.9: Comparison between trace gas emissions from non contaminated and insect contaminated chick peas using CLD technique.

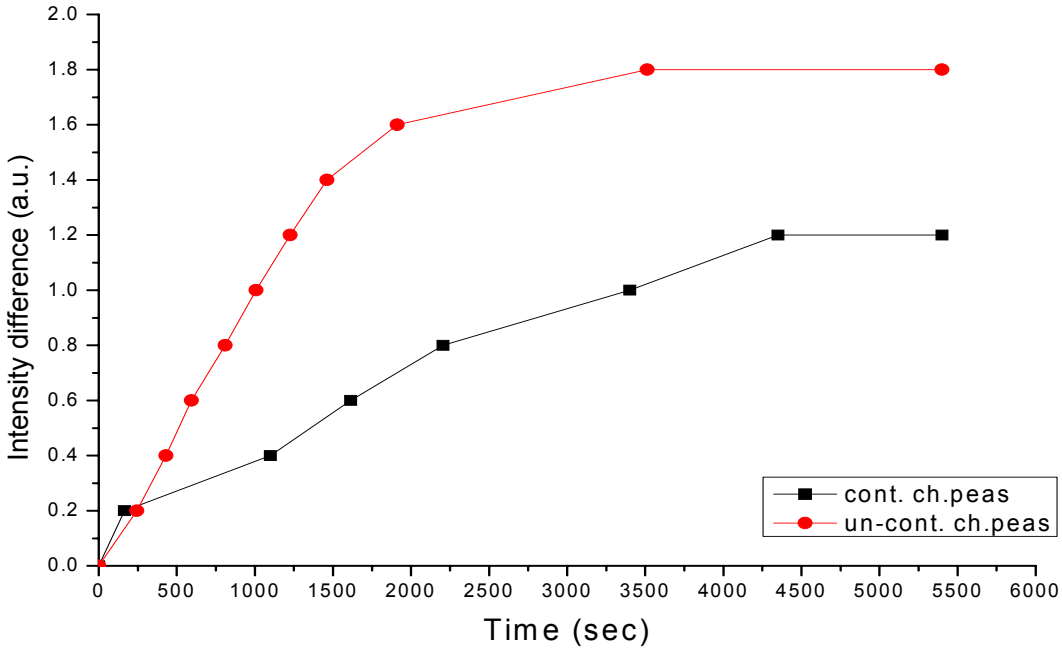

Fig 4.10: Comparison between trace gas emissions from non contaminated and insect contaminated chick peas using PTLD technique.

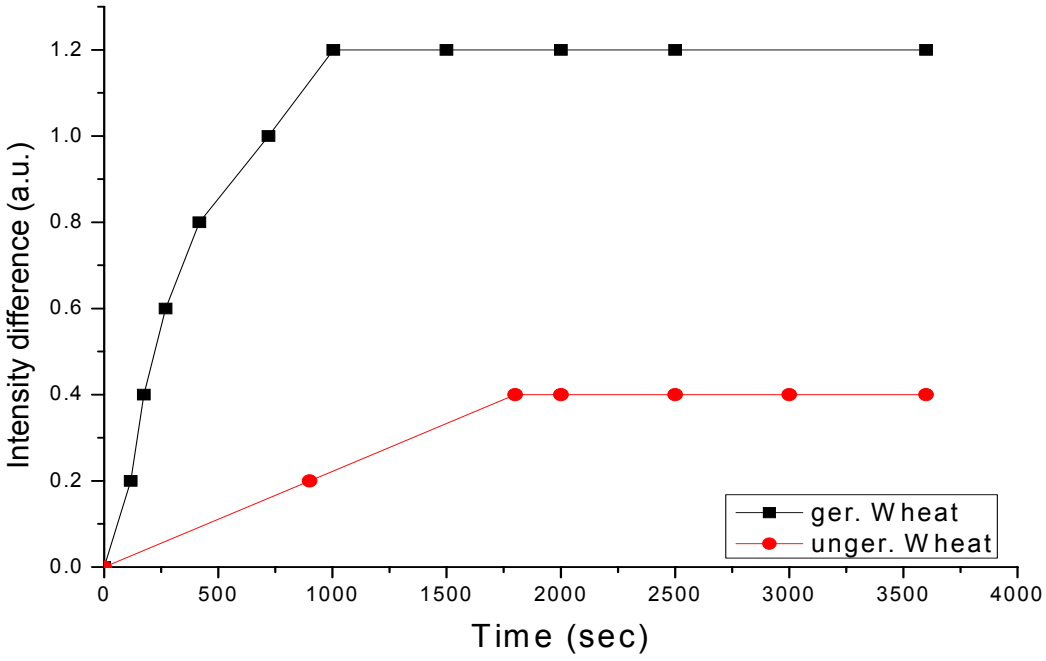

Fig 4.11: Comparison between trace gas emissions from germinated and un germinated wheat grains using CLD technique.

4.5 Comparison between CLD and PTLD techniques.

In the previous sections of this chapter the results of CLD and PTLD were presented. In both techniques the effect of gas traces of different samples that are known (methanol and acetone) or unknown (leaves, flowers and seeds) gas structure were detected. Both techniques proved to be sensitive tools for the detection of gas emissions from samples as small as 20μL of CH3OH and acetone. In the present section a comparison between the use of PTLD and CLD for detection of gas traces employing a deflected laser beam is carried out. These comparison results could help us to identify the technique that is more sensitive than the other. Comparison between the two techniques of Methanol and Acetone results are shown in Figures 4.12a and b. Figures 4.13,4.14 and 4.15 show a comparison between the use of CLD and PTLD techniques to detect trace gases from Mint, jasmine and chick peas respectively. To further prove the technique which is most sensitive is the PTLD technique used to detect trace gas from only one Jasmine flower, see Figure 4.16.

It is believed that each plant leave emit a trace gas that contain part of the gases emitted by its flower. To investigate this fact the relation between gas emissions from jasmine leaves and flowers shown in Figure 418. Finally each technique can also used to compare between the gas emissions from any two different samples; for example Figure 4.19 shows a comparison between the gas emission from 40μl of methanol and 40μl of acetone using CLD technique.

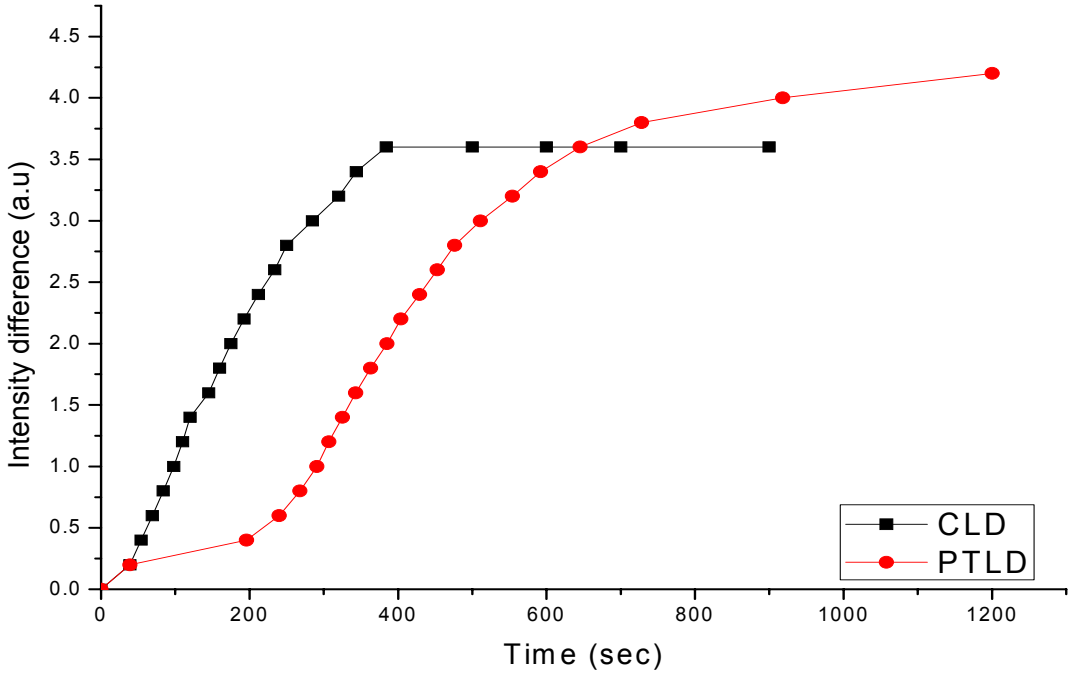

Fig 4.12a: Comparison between the use of CLD and PTLD techniques to detect trace gases from 40µL of Methanol.

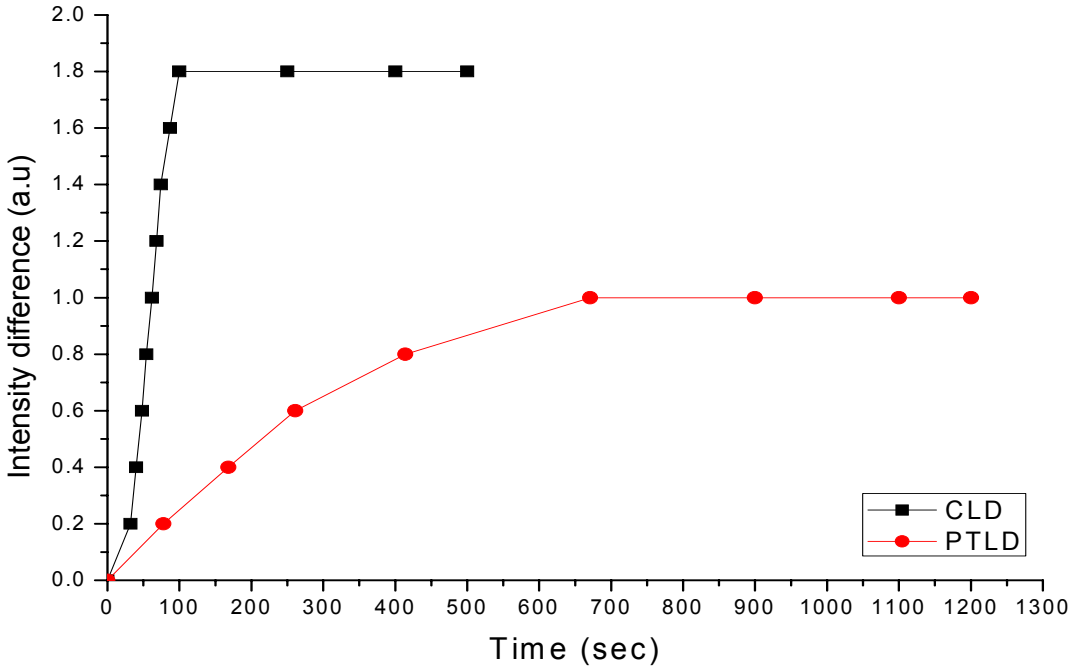

Fig 4.12b: Comparison between the use of CLD and PTLD techniques to detect trace gases from 40µL of Acetone.

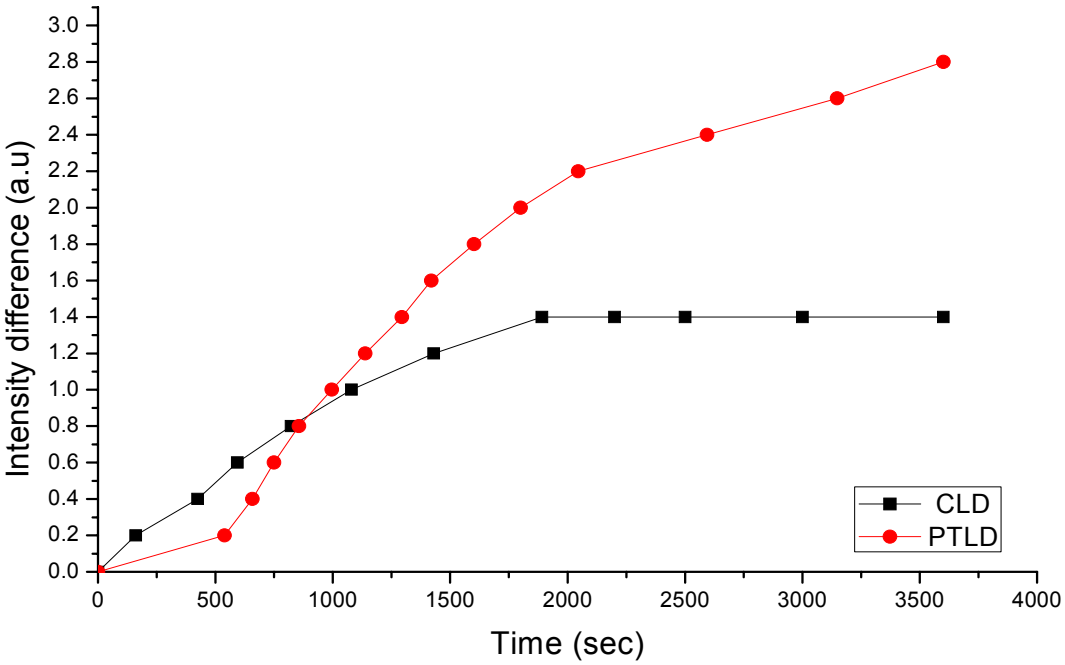

Fig 4.13: Comparison between the use of CLD and PTLD techniques to detect trace gases from 0.25g of mint.

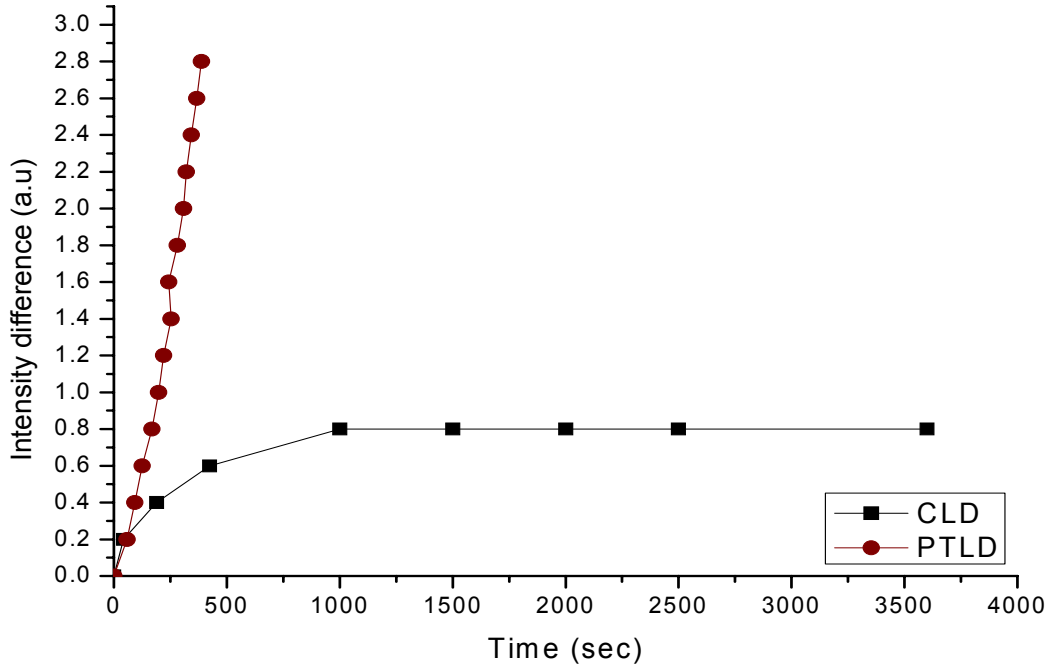

Fig 4.14: Comparison between the use of CLD and PTLD techniques to detect trace gases from jasmine white flower.

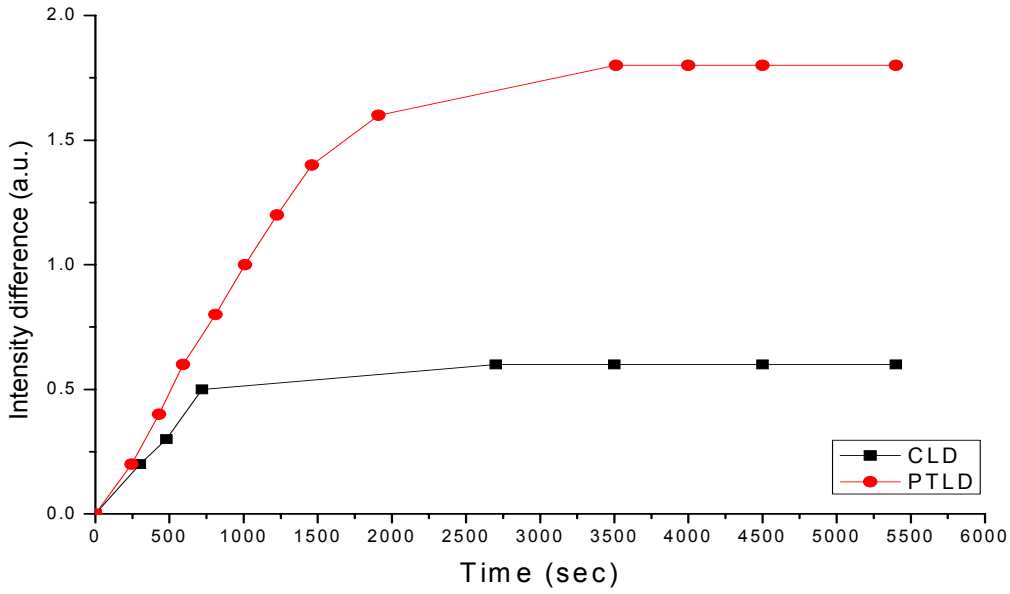

Fig 4.15: Comparison between the use of CLD and PTLD technique to detect trace gases from insect contaminated chick peas.

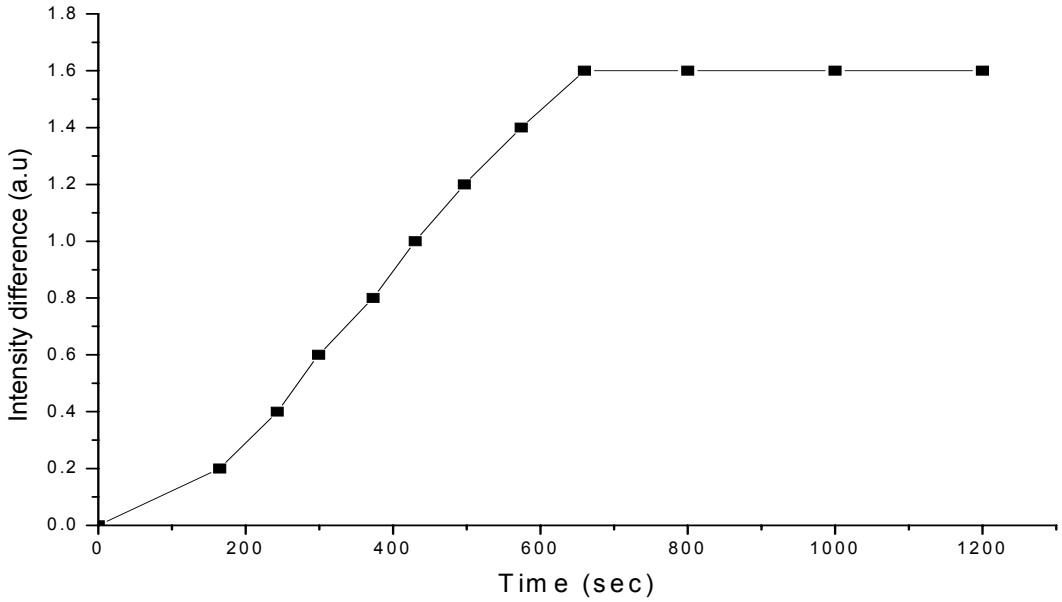

Fig 4.16: Trace gas emissions from one Jasmine white flower using PTLD technique.

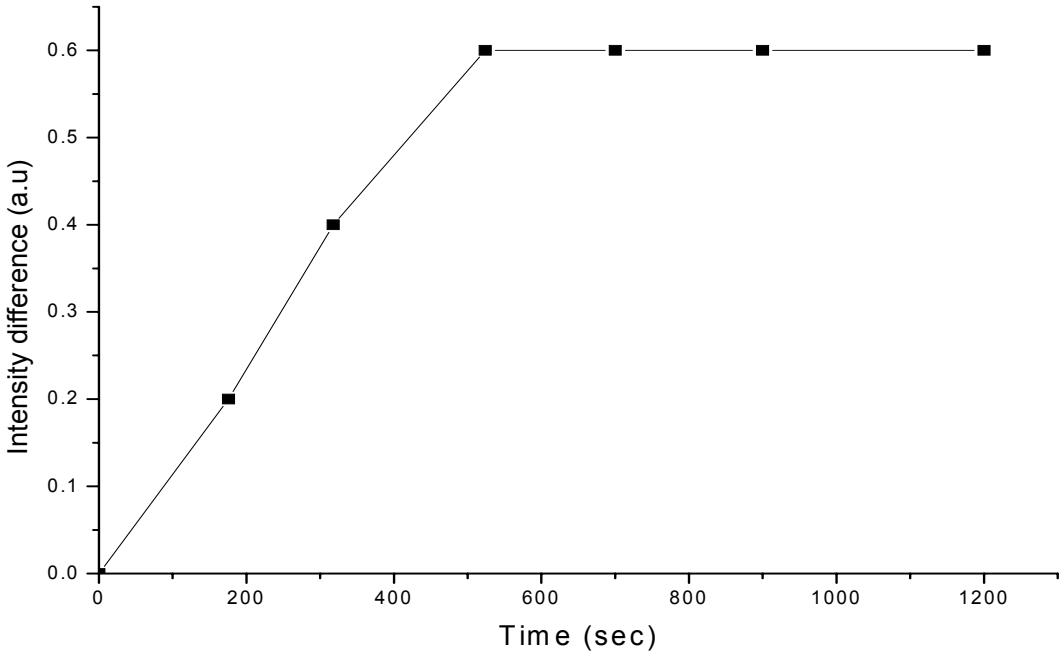

Fig 4.17: Detection of gas trace emission from jasmine's six (o.5g) plants' leaves using PTLD technique.

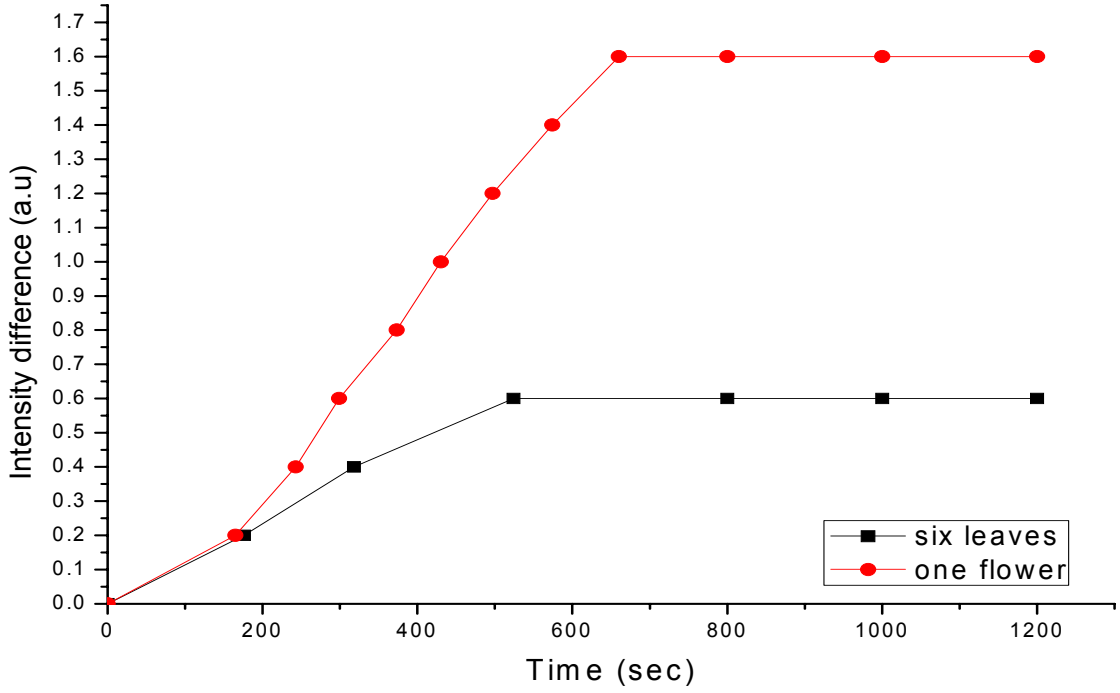

Fig 4.18: Comparison between the gas trace emissions from Jasmine's one flower and Jasmine's six plants' leaves (0.5g) using PTLD technique.

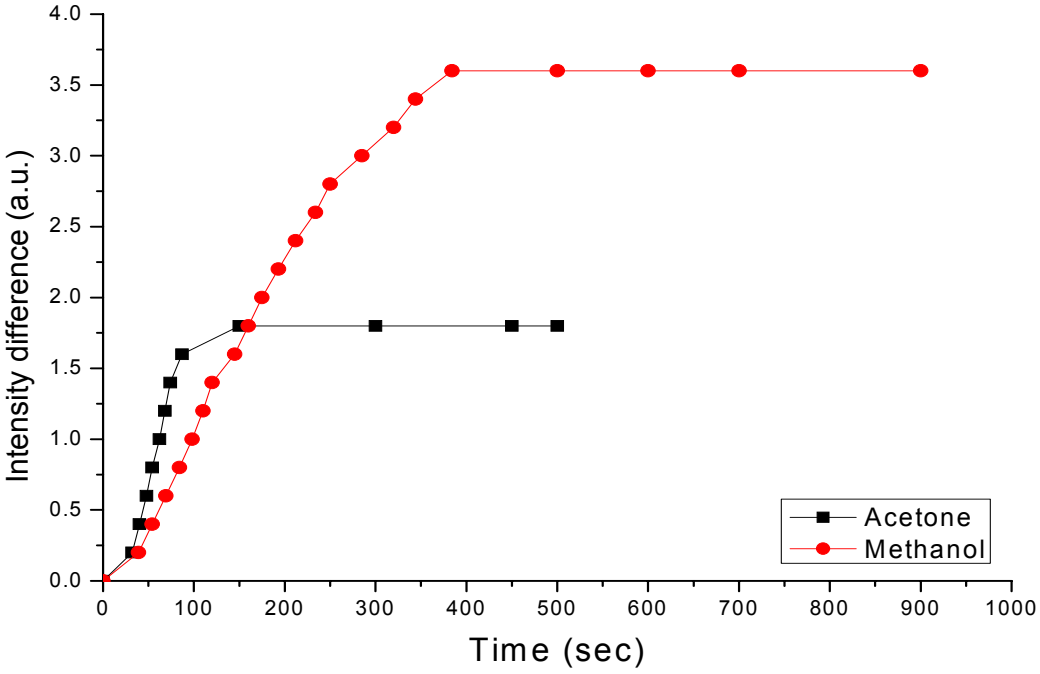

Fig 4.19: Comparison between the gas trace emission from 40µL of acetone and 40µL of methanol using CLD technique.

Chapter Five

Discussion

5.1 Introduction.

In this chapter, the data obtained from the experiment are discussed along three paths; one involves results of known and unknown gas emissions using CLD technique. The second involves results of known and unknown gas emission from samples using PTLD technique. The third involves the comparison between results of CLD and PTLD. Both CLD and PTLD signals were monitored as a function of time. In PTLD experimental part samples were allowed to absorb wideband IR radiation from a pulsed IR source, i.e. for the experiment a probe and a pump beams are used; contrary to CLD technique which involves only one beam namely the probe beam. As mentioned earlier no position sensor of the deflection beams in both techniques were used and instead a diffraction slit proved very useful and satisfactory.

5.2 Conventional light deflection results.

This new less sophisticated technique was used to detect trace gas emissions from different samples. As shown in Figure 3.2 the system used was very simple and inexpensive.

5.2.1 Methanol and Acetone Results:

Methanol is the simplest alcohol, and evaporated at room temperature . Acetone $(CH_3)_2CO$ is the simplest example of the ketones and it is evaporated at room temperature too, but faster than methanol.

Figure 4.1a shows the signal of light intensity difference versus time of different methanol volumes. CH_3OH evaporated with time so by placing a little volume of it's liquid in a closed glass box, it was evaporated piecemeal. By the time the methanol vapor and the concentration of methanol's gas were increased inside the box. Equation (2.8) which shows the effect of gas density on the refractive index (directly proportional). The gas or the evaporation density were increased inside the box with time, so a gradient refractive index would be produced, that effect on the path of laser probe beam. So there would be a gradient in the deflection of the probe beam. This deflection beam passed through a single slit then dropped on a fiber optic on photometer's head.

By increasing methanol's volume the periodic time of evaporation were increased for example 20 µl is completely evaporated faster than 40 µl, and the evaporation rate will increase too. So the signal of small volume becomes constant faster than that of large

volume. i.e. 20 µl of methanol evaporated through 380 seconds while 60 µl evaporated through 620 seconds. The effect of 60 µl of methanol on the probe beam's path is more sensitive (faster) than 40 µl which is more than 20 µl.

The same for acetone; Figure 4.2a shows the signal of light intensity difference versus time of different acetone volumes. Its results were the same as the results of methanol in Figure 4.1a.

From these two results the sensitivity of the present experimental system could be determined.

The box volume = $5 \times 5 \times 4.5 = 112.5\ cm^3 = 112.5 \times 10^{-3}$ liters

The number of air moles in 112.5×10^{-3} liters $= \frac{volume}{22.4} = \frac{112.5 \times 10^{-3}}{22.4} = 5.022 \times 10^{-3}$ moles

The number of air molecules in the box (N_a) $= 5.022 \times 10^{-3} \times 6.022 \times 10^{23} = 30.242 \times 10^{20}$ molecules

And so for the smallest volume of samples (methanol or acetone) were used;

The number of sample moles in 20µL $= \frac{20 \times 10^{-6}}{22.4} = 0.893 \times 10^{-6}$ moles

The number of sample molecules in the box (N_s) $= 0.893 \times 10^{-6} \times 6.022 \times 10^{23} = 5.378 \times 10^{17}$ molecules

The sensitivity of this experimental system $= \frac{N_s}{N_a} = \frac{5.378 \times 10^{17}}{30.242 \times 10^{20}} = 0.178 \times 10^{-3}$

So this system sensitivity is 0.178 molecules per 1000 molecules or 178 per million. This result proves that this system is sensitive and it can detect the gas emission from ≈178 molecules in one million molecules, i.e. 178 part per million (ppm).

To compare the experimental results obtained here with previous experimental work, two issues can be raised: Firstly, the CLD method has never been done before and no results were found for comparison. Secondly, the PTLD method employing position sensor sensitivity it can be as small as 250 ppt (Zimering and Bocarra, 1997).

5.2.2 Leaves results:

Two different masses of mint and sage samples were used. These two leaves have a different gas emission. Figure 4.3a shows the signals of light intensity difference versus time of different masses 0.25g and 0.5g of mint. Because of the gas emission, gas density and the pressure were increased inside a glass box by the time which would be effected by the refractive index of gas inside the box, i.e. a gradient of refractive index were produced with time (equation 2.7) which affect the path of the reflected beam. The position of deflected beam on the fiber optic of photometer's head was shifted along the principle spot, so the reading of light intensity was decreased.

The effect of mass: By increasing the mass of mint and sage, the gas emission density was increased more rapidly and so the pressure inside the box. As Figure 4.3a shows that the signal of 0.5g mint differs more rapidly than 0.25g. The same happened for sage as in Figure 4.5a.

The effect of crushed leaves: The speed and the amount of gas emission could be increased by crushing mint's and sage's leaves so the rate of gas emission would be increased. By crushing mint's and sage's leaves the speed of gas emission was noticed to increase and so a gradient in the refractive index would be produced faster than in the case of uncrushed leaves; this explains rapid increase in the signal of crushed leaves, than it's in the case of uncrushed leaves as shown in Figures 4.3b and 4.5b. These results, since the

refractive index gradient is direct proportional with gas density as in equation 2.7. In the case of crushing leaves the existence of additional components such as water (which also evaporates) must be considered. Crushing mint's or sage's leaves made gas emission easier and faster.

5.2.3 Flowers result:

Jasmine and rose were used in this part; a specific number flower's leaves were taken from both. So the mechanize of this part is as leaves (mint and sage). Two different colors from these two flowers were used, so by this technique the comparison between the gas emissions from the different colors of the same flower were studied. Figure 4.6a shows the signal of Jasmine white and yellow flowers. From this signal, it could be detected that if these two flowers (white and yellow) emit the same kind of gas structure, the rate of gas emission from white Jasmine is more than it is in yellow, in spite of, these flowers of different color were taken from the same plant. Or it could be detected that each color of Jasmine's flower had it's a special refractive index which is different than the other color of the same plant.

The same results detected for white and red rose flower, but these flowers were taken from two different rose's plants. Figure 4.8a shows that the rate of gas emission from red rose is more than that from white rose, if it emits the same kind of gas structure. Or they have a different kind of gas with different refractive index.

The speed and the amount of gas emission will increase by crushing the flowers. Figure 4.6b and Figure 4.8b show that the rate of gas emission would be increased by crushing the flowers. So this system could study the rate of gas emission from the sample. Increasing in the rate of gas emission causes increasing in the gas density inside the box

and a gradient in the refractive index would be produced. So the signal of crushing flowers differed more rapidly than uncrushing flowers.

5.2.4 Seeds results:

Wheat and chick peas were used in this part. The comparison between the gas emission from a healthy and insect contaminated chick peas and from germinated and un germinated wheat could be detected using CLD technique. This means that insect actions in seeds could be detected by this technique. Figure 4.9 show the difference between the signals of healthy and contaminated chick peas. From this Figure it could be concluded that the amount of gas emitted from a healthy chick peas was less than the infected ones. This means that a healthy seed hadn't emitted any gas or it emitted a very little quantity of gas which had no effect on the refractive index. By comparison between the signals of healthy and contaminated chick peas the gas emission from insect decay could be detected.

Figure 4.11 shows the difference between the signals of un germinated and germinated wheat, when wheat become wet it starts to germinate. From Figure 4.11 it could be detected that a gas emission from germinated wheat is more than a gas emission from un germinated wheat, and the existence of additional components such as water, which also has its effect on the signal. So by this technique it could be differentiated between the germinated and the ungerminated wheat.

5.3 PTLD results.

In this part the same samples with the same quantities were used. The only difference from CLD is the use of IR source, i.e. gradient index is initiated by trace gas absorption of IR-radiation. Hence, in photothermal deflection spectroscopy probe beam is deflected due to index change as a result of both gas emission and IR absorption.

5.3.1 Methanol and acetone results:

Methanol (CH_3OH) absorbs in the range "5000 to 667" cm^{-1}, the high frequency libration band of methanol centered at 670 cm^{-1}, shifts to substantially lower frequencies upon dilution, indicating marked changes in the librational motion of the hydroxyl hydrogen of methanol. This band is a sensitive probe of the hydrogen bonding environment experienced by methanol molecules. A methanol bands appear to have attributed to the O - H, C - H, C - O and C – C vibrations within the molecules. A methanol intense absorptions occur near 3704, 2941, 1346, 1333 and 1042 cm^{-1} which are attributed to the O - H and C - H stretching, O - H and C - H bending and C – O stretching vibrations, respectively (Earle and plaler, 1952).

Acetone $(CH_3)_2CO$ picks up water from the air. Therefore, acetone should be capped when not in use. And it absorbs UV light with wavelengths longer than 220 nm. Acetone intense absorptions occur near 2973, 2931, 1702, 1448, and 1363 cm^{-1} which are assigned to the vibrational modes of molecularly absorbed acetone (http://www.springerlink.com/content/223h05853343x561/,March, 20009).

Three different volumes of methanol were used. When 20µl and 40µl of methanol were used all liquid samples were evaporated. But when 60µl was used all methanol liquid sample evaporated in 20 minutes; then methanol vapor began to condensate on the box's walls this results in a decrease in the intensity meter reading. This because the box become saturated with gas molecules so they condensate on the box's walls. Hence the result would be a decreasing in the density of the gas inside the box, i.e. refractive index decrease. This effect was clear when the probe beam deflection reverses to the opposite direction. The same happened for 60µl of acetone. This effect was not noticed in CLD method.

20 µl of acetone couldn't be used since it evaporates very quickly; all liquid samples were completely evaporated through 45 seconds, i.e. needs a recorder to read results. So the reading of intensity versus time couldn't be taken. Figures 4.1b and 4.2b show the signals of light intensity difference versus time for different volumes of methanol and acetone respectively. The deflection angle as given in equations 2.16 and 2.17 depends on the temperature effect of the refractive index $\frac{dn}{dT}$ term and on the density of gas. When samples volume becomes larger, the rate of evaporation would be increased, and the number of gas molecules inside the box which absorbed IR radiation was also increased. The result would be; by increasing Acetone and Methanol volumes, the deflection angle would be changed more quickly. This means; the absorption of 60µl of methanol vapor is greater than that for 40µl which is greater than that for 20µl, and the same for acetone. These all results were shown in Figures 4.1b and 4.2b. For all volumes, the kind of gases were the same CH_3OH or $(CH_3)_2CO$ so IR absorption is the same, but the number of absorbing molecules are increased by time.

5.3.2 Mint results:

In this part green mint leaves were investigated. As in CLD method, two different mint masses were used, and the rate of gas emission increased by crushing mint's leaves.

Figure 4.4a shows trace gases emission from different mint masses were monitored using PTLD technique. The light intensity reading of 0.5g was changed faster than that for 0.25g. In both cases mint emitted the same kind of gas species put with different quantity. At the same period of time the rate of gas emitted measured as an absorption of IR radiation by the 0.5g is greater than that from 0.25g, since gas emission rate is directly proportional to mass of mint leaves. Therefore, absorption by 0.5g of mint is greater than that by 0.25g; these results were noted in Figure 4.

In Figure 4.4b the rate of gas emission were increased not by increasing the sample's mass as in Figure 4.4a, but by crushing the sample's maxinti. The same results were noted, but in this case the existence of additional components must be considered. For example when mint's leaves were crushed the existence of water vapor is expected to be greater than when leaves are not crushed. Water is the main absorber of the sunlight and shows strong absorption in the infrared region. In the gas phase it absorbs in the regions 3657, 3755, 1594 cm^{-1} (http://www.Isbu.ac.uk./water/index2.htm,march 2009). The time needed to reach the saturation for crushed leaves is less than that for un crushed leaves; this is enhanced by the release of gas molecules as the sample is crushed.

5.3.3 Flower (jasmine) results:

White and yellow flowers from the same Jasmine plant were used. Figure 4.7 shows a comparison between the gas emissions from white and yellow Jasmine's flower using PTLD technique. Results were similar to those of mint in CLD part, i.e. rate of gas emission is directly proportional to the mass used.

Figure 4.7 shows that there was a difference between these two colors of the same Jasmine plant. If these two flowers (white and yellow) emit the same kind of gas structure, the rate of gas emission from white Jasmine is more than that from yellow one, i.e. at the same period of time the number of gas molecules emitted from white flowers and absorbed IR radiation was greater than that in yellow flowers, so as seen in Figure 4.7 the white signal different is faster than yellow signal. Or it could be detected that white and yellow Jasmine's flower have different kinds of gas species and each has it's absorption range of IR radiation, white absorption greater than yellow absorption.

In Figure 4.17 the trace gas emission from Jasmine's green leaves were monitored. From these results, it could be detected that; also Jasmine's leaves emit gas that absorb in the IR region radiation which affect the refractive index, hence, producing a beam angular deviation. In Figure 4.18 the trace gas emission from one jasmine’s flower were detected, this proves the sensitivity of our system since it could monitor gas traces emitted from only one flower (0.15g).

5.3.4 Chick peas results:

Figure 4.10 Shows that by using PTLD technique a gas emission from insect activities could be detected. When insects contaminated chick peas used as a sample the signal changed faster than the signal of non contaminated chick peas. The existence of alive insect with their action affect the rate of gas emitted in side the box, then on the absorption of IR radiation. For example these insects breath so they exchange gases inside the box. In this case the kind of gases that are emitted from the chick peas differ than that emitted from healthy chick peas, and these gas absorptions are greater than that in the healthy seeds. So by these two systems it could be differentiated between contaminated and non contaminated seeds.

5.4 Open area results.

In this part the simple CLD method were used to detect an emitted smoke from one cigarette placed such that its smoke is flown across the path of the laser beam. The effect of air speed purring brought the path of the laser beam were investigated too.

The laser beam allowed to fall on a mirror fixed on the wall inside the lab room, and then the reflected beam was allowed to pass through slit and then dropped onto the fiber optic of the photometer's head, on the center of the principle spot as in previous parts. The light intensity reads were noted. It was found that the CLD method is applicable for both smoke detection and changes of air speed in the form of draft. For example for the case of air draft blown in the beam indicated a change from 8 arb. intensity unites to 2 a.us. When draft is flown from the opposite side deflection is from 2 – 8 a.us. This application indicates the tendency of the method for open area applications, for example detecting insect sprays in moving winds across insecticide sprayed fields.

5.5 Comparison results.

Figures 4.12a, 4.12b, 4.13, 4.14, and 4.15 were used to compare between the use of CLD and PTLD techniques in detecting trace gases emitted from different samples. From these Figures the following conclusions could be drawn:

- PTLD technique is more effective and sensitive than CLD technique.
- CLD is in expensive, easy to handle and has a wider use than PTLD.
- By comparing the results of the two techniques the extent of IR absorption by gas sample can be recognized.
- Because of the sensitivity of PTLD technique it could be used to detect gas traces of very small quantities of samples that have absorption to IR radiation.
- It could be detected that the rate of gas emission from the flower is more than that from the same flower leaves, and it could be detected that the rate of gas emission from acetone is more than from methanol (at the same periodic of time).
- Although the CLD is less sensitive from the PTLD, it can be used widely in many applications, this is enhanced by its simplicity and independence of an absorption line, contrary to the PTLD which relies heavily on the existence of an absorbing species for detection.

Chapter 6

Conclusion and further work

6.1 Conclusions.

A set of this experiment was performed successfully using two simple, sensitive, easy to handle, safely, inexpensive and accurate systems. In this chapter concentration will be focused on the basic conclusions of this work. One important conclusion can be drawn from the use of CLD and PTLD methods to detect gaseous species at the trace level for different samples. This experiment proved the ability of the two methods to distinguish different kinds of samples at 178 part per million (ppm). Both methods were used without the need for position sensor, instead a slit was used. This is considered an achievement for such experiments, resulting in the enhance of their use.

The present work proved that an expensive position sensor could be replaced successfully with a single diffraction slit. The newly suggested CLD could be improved for sensitivity and both CLD and PTLD methods are very useful tools for trace gas detection, but with different sensitivities, advantages and disadvantages.

Using CLD and PTLD techniques to test different samples such as seeds, flowers and leaves have the following conclusions.

1- It proved a good possibilities of using CLD and PTLD method to detect trace gases; leading to many important applications.
2- This experiment proved the ability to distinguish a very little quantity of different samples, i.e. 20µl of methanol (5.4×10^{17} molecules), one jasmine's flower,…etc.
3- It's proved that an expensive position sensor could be exchanged with inexpensive equipment; i.e. single slit and a photometer.
4- The distance that a deflection beam was shifted can be determined by comparing each graph of intensity versus time (in chapter four) with Figure 3.1.
5- In agriculture these two techniques opens a wide area of applications. These techniques can distinguish between healthy and unhealthy plants as in chick peas and wheat. This can be satisfied by having Figure of intensity differs through a periodic of time as a finger print of each sample.

6.2 Further work

The PTLD method is a well known and comprehensively study for variety of applications. The newly suggested method CLD still needs a more through investigation as far as sensitivity is concerned. Other applications using the new method could be suggested and studied; a cortile region for such work is in environmental monitoring.

References:

- Aamodt, L., Murphy, J. (1982): "Effect of 3-D heat flow near edges in photothermal measurements", applied optics, 1. 111-115.
- Abu-Taha, M.I. (2008) Private communications, physics Dept. Al-Quds University, Jerusalem, mabutaha@ science. alquds.edu.
- Arendt, J., R. (1989): Introduction to classical and modern optics, 3rd ed., Prentice Hall, New Jersey.
- Bailey, R., and Cruickshank, F. (1989): Thermal lensing, Photoacoustic, Photothermal, and Photochemical in Gases, Springer-Verlag, Berlin.
- Bertolottii, M. and et al (1993): "On the photo deflection method applied to low thermal diffusivity measurements". Rev. Sci. Instrum, 6. 1576 – 1583.
- Bialkowski, S.E.(1996): Photothermal spectroscopy methods for chemical analysis,Utah State University, USA.
- Bialkowski, S.E. (1998): "Progress toward a better understanding of signal generation in laser-excited photothermal spectrometry of homogeneous samples". Trends in analytical chemistry, 520 –531.
- Boccara, A., Fournier, D. (1980): "Sensitive photothermal deflection technique for measuring absorption in optically thin media". Optics Letters, 9. 377 – 379.
- Bohren C., Huffman D. (1983): Absorption and scattering of light by small particles, John Wiley, New York.
- Born, M., Wolf, E. (1999): Principle of optics, 7th ed., Pergamon press Ltd, London.

- Calasso, I.G. (1998): Photoacoustic and Photothermal Laser Spectroscopy Applied to Trace Gas Detection and Molecular Dynamics، Diss. ETH No. 12925, Zurich, Italy.
- Chen, Y., and et al (1993): "Photo induced absorption studied by photothermal deflection spectroscopy: Its application to the determination of the energy of dangling- bond states in a-Si: H". Chinese journal of physics, 6. 390 -396.
- Coufal, H. (1990): "Photothermal spectroscopy and its analytical application". Freseniual J. Anal Chem., 337. 835 - 842.
- De Vries H. and et al (1992): The photothermal deflection technique (pdt): fast trace gas detection in the atmosphere. In: Bicanic D. (ED.) Photoacoustic and photothermal phenomena III, Springer-Verlag, Berlin, Heidelberg.
- Earle, Plyler, 1952, Ir spectra of Methanol, Ethanol, and rezpropanol, pp 281 – 286.
- Gotoh, T., and et al. (1997): "Photothermal bending spectroscopy and photothermal deflection spectroscopy of C_{60} thin films", applied surface science, 114. 278 – 281.
- Freeman, M.H. (1934): Optics, 10^{th} ed. MPG book Ltd, London.
- Gunzler, H., Gremlich, H. (2002): IR spectroscopy, Federal Republic, Germany.
- Jenkins, F.A, Whith, H.E. (1937): Fundamentals of optics, forth edition. Mc Graw Hill book, USA.
- Halliday, D., Resnick, R. (1981): Fundamentals of physics, 2^{nd} ed., John Wiley and sons, Canada.
- Havaux, M., and et al. (1989):" Photothermal beam deflection: a new method for in vivo measurements of thermal energy dissipation and photothermal energy conversion in intact leaves", Photosynthesis research, 24. 63 – 73.

- Henrik, A. (2008): Position Sensitive Detectors - Device Technology and Applications in Spectroscopy, Mid Sweden University, Sweden.
- Klien, M., Furtak, T. (1933): Optics, 2nd ed., Canada.
- Kosmovskii, S., and et al (1998), "Biomedical Engineering". 3.
- Laine, D., et al (1997): Optoelectronics, IEE Proceedings, 5. 315 – 322.
- Lajunen, L.H. (1992): Spectrochemical analysis by atomic absorption and emission, royal society of chemistry, Great Britain.
- Malik, A., Faubel, W. (2000): "Photothermal and light emitting diodes for trace detection in capillary electrophoresis". Chem. Soc. Rev., 29. 275 – 282.
- Massari, N., and et al (2002): "High Speed Digital CMOS 2D Optical Position Sensitive Detector", Trento, Italy.
- Minnaert, M.G. (1974): Light and color in the outdoors, fifth ed., Springer-Verlag, New York.
- Murphy, J., Aamodt, L. (1980): "Photothermal spectroscopy using optical beam probing: Mirage effect". Applied physics, 9. 4580 - 4588.
- Pitz, R. (1990): Low level smoke emission measurements from a flame by photothermal deflection spectroscopy". Applied optics, 16. 2418 -2423.
- Ravi, J., and et al. (2002): Asimple theoretical extension to the analysis of photothermal deflection signal for low thermal diffusivity evaluation". Quantitave spectroscopy and radiative transfer, 83, 193 – 202.
- Salazar, A, and et al (1993): "thermal diffusivity measurements on solids using collinear mirage detection". Appl. Phys., 3. 1539 – 1547.
- Sears, F.W. (1949): Optics, 3rd ed., Addison-Wesley, London.
- Sell, J. (1985): Gas velocity measurements using photothermal deflection spectroscopy". Applied optics, 22. 3725 – 3735.

- Shi, B., and et al. (1999): Measurements of thermal diffusivity of boron-silicon film-on-glass structure using phase detection method of photothermal deflection spectroscopy", materials science, 34. 5169 – 5173.
- Spear, J. and et al (1990): "Collinear photothermal deflection spectroscopy with light-scattering samples". Applied physics, 28. 4225 – 4234.
- Spear, J.D. and et al (1998): "Photothermal deflection spectroscopy of an aqueous sample in a narrow bore quartz capillary". Review of scientific instruments, 6. 2259 - 2265.
- Stover, J.C. (1995): Optical Scattering: measurement and analysis, 2nded, The international society for optical engineering, USA.
- Taubenblatt, M. (1988): Photothermal absorption microprobe: infrared spectroscopy of a single 1μm organic particle". Appl. Phys. Lett, 12. 951 – 953.
- Young, H.D. (1992): Extended version with modern physics, 8th ed., Addison-Wesley published company, USA.
- Zimering, B. and et.al (1997): "Photophysical and photocomposition studies on polyethylenes: A novel application of gas-phase mirage-effect spectroscopy". Applied Polymer science, 1875 – 1883.

Internet Sites:

- Aculux, LLC 500-0005-003, 55-116 th Ave NE, Suite 117, 01/04 Bellevue, WA 98004 (425) 378-0567 ● info@aculux.com.
- http://www.springerlink.com/content/j137743836330278/, april 2009.
- http://micro.magnet.fsu.edu/primer/java/diffraction/basicdiffraction, December200.
- http://en.wikipedia.org/wiki/Dynamic_light_scattering, December, 2008.
- http://www.nsg.co.jp/en/it/c2/lens/tlm.html, April 2009.
- http://www.fceia.unr.edu.ar/fisicaexperimentalIV/Pasco/High%20sensitivity%20photometer, December 2008.
- http://en.wikipedia.org/wiki/Methanol, December, 2008.
- http://en.wikipedia.org/wiki/Acetone, December, 2008.
- http://www.springerlink.com/content/223h05853343x561/, March, 20009.
- http://www.Isbu.ac.uk./water/index2.htm,march 2009.